TKK Dissertations 225
Espoo 2010

LES OF CERTAIN DROPLET SIZE EFFECTS IN FUEL SPRAYS

Doctoral Dissertation

Ville Vuorinen

Aalto University
School of Science and Technology
Faculty of Engineering and Architecture
Department of Energy Technology

TKK Dissertations 225
Espoo 2010

LES OF CERTAIN DROPLET SIZE EFFECTS IN FUEL SPRAYS

Doctoral Dissertation

Ville Vuorinen

Doctoral dissertation for the degree of Doctor of Science in Technology to be presented with due permission of the Faculty of Engineering and Architecture for public examination and debate in Auditorium K3/118 at the Aalto University School of Science and Technology (Espoo, Finland) on the 29th of May 2010 at 12 noon.

Aalto University
School of Science and Technology
Faculty of Engineering and Architecture
Department of Energy Technology

Aalto-yliopisto
Teknillinen korkeakoulu
Insinööritieteiden ja arkkitehtuurin tiedekunta
Energiatekniikan laitos

Distribution:
Aalto University
School of Science and Technology
Faculty of Engineering and Architecture
Department of Energy Technology
P.O. Box 14300 (Puumiehenkuja 5 A)
FI - 00076 Aalto
FINLAND
URL: http://www.aalto.fi
Tel. +358-9-470 23460
Fax +358-9-470 23454
E-mail: ville.vuorinen@tkk.fi

ISBN 978-952-60-3165-1
ISBN 978-952-60-3166-8 (PDF)
ISSN 1795-2239
ISSN 1795-4584 (PDF)
URL: http://lib.tkk.fi/Diss/2010/isbn9789526031668/

TKK-DISS-2762

Multiprint Oy
Espoo 2010

Aalto University

ABSTRACT OF DOCTORAL DISSERTATION	AALTO UNIVERSITY SCHOOL OF SCIENCE AND TECHNOLOGY P.O. BOX 11000, FI-00076 AALTO http://www.aalto.fi

Author Ville Anton Vuorinen

Name of the dissertation

LES of Certain Droplet Size Effects in Fuel Sprays

Manuscript submitted 09.09.2009	Manuscript revised 05.05.2010

Date of the defence 29.05.2010

☐ Monograph ☒ Article dissertation (summary + original articles)

Faculty	Faculty of Engineering and Architecture
Department	Department of Energy Technology
Field of research	Fluid Mechanics (Computational Fluid Dynamics)
Opponent(s)	Prof. Franz Tanner and Tellervo Brandt, D.Sc. (Tech.)
Supervisor	Prof. Martti Larmi
Instructor	Prof. Laszlo Fuchs and Ossi Kaario, D.Sc. (Tech.)

Abstract

This thesis belongs to the field of mechanical engineering, more precisely to computational fluid dynamics and fuel injection modelling. This type of problems have been extensively studied because of their practical importance, for example, in combustion processes of automotive industry. Novel challenges are reduction of exhaust gas emissions in the present diesel fuel-based and also in bio diesel-based concepts.

The problem studied in this work is of generic nature and it can be related to many real world problems. A model problem of droplet-laden jet is studied to emulate a fuel spray. The most essential parameter that is studied is fuel droplet size. More precisely, the ratio of droplet timescale and fluid timescale i.e. the Stokes number.

Mathematically, the studied system can be formulated in terms of the Navier-Stokes equation with a spray momentum source term at low Mach number regime. A feature characteristic to this study is to use large scale computer simulation to simulate the system. For adequate modelling, this work makes use of a method called Large-Eddy Simulation (LES) to simulate the motion of the turbulent gas and Lagrangian Particle Tracking (LPT) to simulate the motion of the droplets. The main computational tool used in this work is the OpenFOAM software. In fact, the present work is one of the first computational studies on LES/LPT diesel spray modeling in which droplet-level phenomena are discussed in light of the global behavior of the spray jet in an extensive manner.

In view of the literature on this topic the results of the work seem to be realistic. The dependence of spray shape on droplet size (Stokes number) is studied and differences between the shapes are consistently explained. It is noted that mixing inside the spray depends significantly on the fuel droplet size. Quantitative and statistical analysis methods are developed in order to explain the connection between spray shape and mixing. The presented analysis explains the results and, on its behalf, the analysis explains the practical observation on the decrease of soot emissions together with decreasing nozzle diameter and increasing injection pressure.

Keywords Droplet size, Mixing, Sprays, OpenFOAM, Large-Eddy Simulation

ISBN (printed) 978-952-60-3165-1	ISSN (printed) 1795-2239
ISBN (pdf) 978-952-60-3166-8	ISSN (pdf) 1795-4584
Language English	Number of pages 120+145

Publisher Aalto University, Department of Energy Technology

Print distribution Aalto University, Department of Energy Technology

☒ The dissertation can be read at http://lib.tkk.fi/Diss/2010/isbn9789526031668

Aalto-yliopisto

VÄITÖSKIRJAN TIIVISTELMÄ	AALTO-YLIOPISTO TEKNILLINEN KORKEAKOULU PL 11000, 00076 AALTO http://www.aalto.fi

Tekijä Ville Anton Vuorinen

Väitöskirjan nimi

Polttoainepisaran halkaisijan vaikutuksesta sprayn muotoon käyttäen suurten pyörteiden menetelmää

Käsikirjoituksen päivämäärä 09.09.2009	Korjatun käsikirjoituksen päivämäärä 05.05.2010
Väitöstilaisuuden ajankohta 29.05.2010	
☐ Monografia	☒ Yhdistelmäväitöskirja (yhteenveto + erillisartikkelit)

Tiedekunta	Insinööritieteiden ja arkkitehtuurin tiedekunta
Laitos	Energiatekniikan laitos
Tutkimusala	Virtausmekaniikka (laskennallinen virtausmekaniikka)
Vastaväittäjä(t)	prof. Franz Tanner ja TkT Tellervo Brandt
Työn valvoja	prof. Martti Larmi
Työn ohjaaja	prof. Laszlo Fuchs ja TkT Ossi Kaario

Tiivistelmä

Väitöskirja kuuluu konetekniikan aihepiiriin, tarkemmin sanottuna laskennallisen virtausmekaniikan tutkimusalaan ja polttoaineruiskutuksen mallintamiseen. Tämänkaltaisten ongelmien ymmärtäminen on saavuttanut viime aikoina paljon mielenkiintoa johtuen niiden käytännönsovelluksista esimerkiksi autoteollisuuden piirissä. Alan suuria haasteita ovat esimerkiksi dieselmoottoreiden päästöjen pienentäminen nykyisissä ja tulevaisuuden moottoreissa.

Väitöskirjassa tutkittava ongelma on luonteeltaan varsin geneerinen ja sen voidaan katsoa liittyvän moniin käytännön ongelmiin. Malliprobleemana tutkitaan ilmasuihkua, jonka seassa polttoainepisarat sekoittuvat muodostaen sprayn. Väitöskirjassa kyseinen ongelma kytketään polttoainesuihkuihin. Tärkein tutkittavista parametreistä on polttoainepisaran halkaisija. Tämä puolestaan voidaan ilmaista kahden aikaskaalan, polttoainepisaran liikemäärän relaksoitumisajan ja integraaliaikaskaalan, suhteena eli nk Stokesin lukuna.

Tutkittavaa systeemiä voidaan kuvata matemaattisesti alhaisen Machin luvun Navier-Stokesin yhtälöllä, jossa on mukana polttoainepisaroista aiheutuva liikemäärälähdetermi. 3D-yhtälöt diskretoidaan ja niiden dynamiikkaa simuloidaan supertietokoneella. Työssä hyödynnetään nk LES-menetelmää (Large-Eddy Simulation), jolla simuloidaan turbulentin kaasun pyörteily ja vastaavasti LPT-menetelmää (Lagrangian Particle Tracking), jolla simuloidaan pisaroiden liike. Tärkeimpänä laskentatyökaluna työssä sovelletaan OpenFOAM-ohjelmistoa. Kyseinen tutkimus on eräs ensimmäisistä laskennallisista LES/LPT-menetelmillä tehdyistä tutkimuksista, missä käsitellään laajamittaisesti diesel-suihkun ilmiömaailmaa kytkien pisaratason ilmiöt suihkun globaaliin käyttäytymiseen.

Aiemman kirjallisuuden valossa voidaan todeta, että työn tulokset vaikuttavat realistisilta. Työssä tarkastellaan erityisesti polttoainesuihkun muotoa pisarakoon (Stokesin luvun) funktiona ja selitetään eroavaisuudet monipuolisen data-analyysin avulla. Työssä havaitaan, että sekoittuminen polttoainesuihkun sisällä riippuu olennaisesti polttoainepisaran halkaisijasta. Työssä kehitetään kvantitatiivisia ja tilastollisia menetelmiä sekoittumisen ja suihkun muodon välisen yhteyden selittämiseksi.

Asiasanat Droplet size, Mixing, Sprays, OpenFOAM, Large-Eddy Simulation

ISBN (painettu) 978-952-60-3165-1	ISSN (painettu) 1795-2239
ISBN (pdf) 978-952-60-3166-8	ISSN (pdf) 1795-4584
Kieli englanti	Sivumäärä 120+145

Julkaisija Aalto yliopisto, Energiatekniikan laitos

Painetun väitöskirjan jakelu Aalto yliopisto, Energiatekniikan laitos

☒ Luettavissa verkossa osoitteessa http://lib.tkk.fi/Diss/2010/isbn9789526031668

Preface

This thesis was completed in the Internal Combustion Engine Research Group at the Helsinki University of Technology (TKK) between January 2005 and May 2010. During the academic year 2006-2007, I worked at the Royal Institute of Technology (KTH) in Stockholm.

I wish to thank my teachers and supervisors from the past years of school, studies and research. I am very grateful to my instructor Prof. Martti Larmi for giving me the challenging research topic of better explaining fuel spray dynamics and providing me the wonderful facilities to complete the project. Prof. Larmi is also the person who pointed out that Large-Eddy Simulation is the future method that will bring more insight to the simulation of turbulent flows. I appreciate the extraordinary chance to get to work with such novel simulation methods and to get to practice my physics skills on the widest possible scale during this thesis. I am also very grateful to my supervisor from TKK, Ossi Kaario, D.Sc.(Tech.), for collaboration, continuous interest, outstanding support and good comments regarding my work.

I sincerely thank my other supervisor Prof. Laszlo Fuchs for guiding me at KTH and for his time in general. Our collaboration, together with the chance to learn to use the OpenFOAM software at KTH, formed the core part of this thesis.

I sincerely thank the pre-examiners Prof. Franz Tanner (Michigan University of Technology) and Joseph Oefelein, Phd. (Sandia National Laboratories) for careful checking of the manuscript as well as constructive feedback.

Many thanks to all my colleagues. In specific, the discussions with Harri Hillamo, M.Sc.(Tech.) and Mika Nuutinen, M.Sc.(Tech.) regarding sprays and turbulence

were a great source of motivation. The assistance given by one of the co-authors, Eero Antila, M.Sc.(Tech.), in the beginning of this thesis was of great help. Many thanks also to our secretary Mrs. Seija Erander-Luukkanen and computer administrator Mr. Olli Ranta for making the everyday life easier! I wish to thank also Mrs. Nyberg for the cozy accomodation in Stockholm and the discussions in Swedish.

My parents, Matti and Sinikka, have always encouraged and supported me. My friends have been of great support during writing the thesis. A special word is reserved for Katja for the ever-lasting presence during the most intensive times.

I thank Mikko Auvinen, M.Sc., Ville Tossavainen, M.Sc.(Tech.), and Esko Järvinen, Lic.Sc.(Tech.) for collaboration in organizing the OpenFOAM basic courses during the years 2008-2009. It has been a pleasure to work with them! I wish to recognize the importance of the OpenFOAM software in making this work possible. I hereby express my most sincere appreciation to all those who have contributed to the OpenFOAM project and wish to share their precious work with the others. The computational resources were provided by CSC-IT Center for Science (Espoo) and PDC (Stockholm). I wish to thank the kind personnel at these computing centers for their support.

The financial help from the Finnish Cultural Foundation, the Henry Ford Foundation, Tekniikan Edistämissäätiö, the Finnish Funding Agency for Technology and Innovation (TEKES) and the Finnish Graduate School of Energy Technology is deeply acknowledged.

Otaniemi, May 11^{th}, 2010

Ville Anton Vuorinen

Contents

List of Publications

This thesis consists of an overview and of the following publications which are referred to in the text by their Roman numerals.

I Vuorinen V., Larmi M., Antila E., Kaario O., El-Hannouny E. and Gupta S., *Near Nozzle Diesel Spray Modeling and X-Ray Measurements*, SAE Technical Paper Series 2006-01-1390, (2006).

II Vuorinen V., Larmi M. and Fuchs L., *Large-Eddy Simulation of Spray-Originated Turbulence Production and Dissipation*, S4_Tue_A_14, Proceedings of the 6th International Conference on Multiphase Flow, ICMF-2007, Leipzig, Germany, ISBN 978-3-86010-913-7, (2007).

III Vuorinen V., Larmi M. and Fuchs L., *Large-Eddy Simulation on the Effect of Droplet Size Distribution on Mixing of Passive Scalar in a Spray*, SAE Technical Paper Series 2008-01-0933, (2008).

IV Vuorinen V., Larmi M. and Fuchs L., *Large-Eddy Simulation of Particle Size Distribution Effects on Turbulence in Sprays*, AIAA-2008-0514, Proceedings of the 46th AIAA Aerospace Sciences Meeting and Exhibit, Grand Sierra Resort, Reno, ISBN 978-1-60560-201-1, (2008).

V Vuorinen V., Hillamo H., Nuutinen M., Kaario O., Larmi M. and Fuchs L., *Effect of Droplet Size and Atomization on Spray Shape: A Priori Study Using Large-Eddy Simulation*, accepted for publication from the best papers of the 6th International Symposium on Turbulence, Heat and Mass Transfer, Rome (2009), into a special edition of Flow, Turbulence and Combustion (09.05.2010).

VI Vuorinen V., Hillamo H., Nuutinen M., Kaario O., Larmi M. and Fuchs

L., *Large-Eddy Simulation of Droplet Stokes Number Effects on Turbulent Spray Shape*, Atomization and Sprays, **20**, 2, 93-114, (2010).

VII Vuorinen V., Hillamo H., Nuutinen M., Kaario O., Larmi M. and Fuchs L., *Large-Eddy Simulation of Droplet Stokes Number Effects on Mixture Quality in Fuel Sprays*, accepted for publication in Atomization and Sprays (05.05.2010).

Author's contribution

In all the Publications V.Vuorinen is the first author. Publication I was initiated by M.Larmi and the experimental part was carried out by E.El-Hannouny and S.Gupta at the *Argonne National Laboratories*. However, the data analysis and numerical simulations were carried out by Vuorinen. The simulations of Publications II-VII were fully designed, carried out and post-processed by Vuorinen. This required extensive utilization of the OpenFOAM software in parallel computing environments and creation of a new CFD-solver code capable for doing LES+LPT using the OpenFOAM software. This code is based on the existing standard solvers of OpenFOAM. Furthermore, a large part of the experiments was to create the rather large data bases for post-processing which was done by Vuorinen. Vuorinen also improved the spray visualization by creating a new algorithm for the visualization purposes of Publications V-VII. Vuorinen also designed and implemented the stochastic droplet breakup model that was introduced and used in Publication V. The experimental diesel spray images in Publications VI and VII were carried out by H.Hillamo.

List of Abbreviations

BC	Boundary Condition
CFD	Computational Fluid Dynamics
CG	Conjugate Gradient
DI	Direct Injection (Engine)
DNS	Direct Numerical Simulation
DRT	Droplet Residence Time
EOI	End of Injection
FOAM	Field Operation and Manipulation
FVM	Finite Volume Method
GD(M)	Gradient Diffusion (Model)
HCCI	Homogenous Charge Compression Ignition
ICP(B)CG	Incomplete Cholesky Preconditioned (Bi-)Conjugate Gradient
ILES	Implicit Large-Eddy Simulation
KH	Kelvin-Helmholtz
LES	Large Eddy Simulation
LPT	Lagrangian Particle Tracking
MG	Multigrid
NOx	A generic term for mono-nitrogen oxides (NO and NO2).
NS	Navier-Stokes
PDE	Partial Differential Equation
PDF	Probability Density Function
PIV	Particle Image Velocimetry
PLJ	Particle Laden Jet - a commonly used name for a jet with particles
PLJM,PLJP	Particle Laden Jet with Monodisperse/Polydisperse particles

PSD	Power Spectral Density
RANS	Reynolds Averaged Navier-Stokes
RMS	Root Mean Square
RHS	Right Hand Side
SGS	Subgrid Scale
SMD	Sauter Mean Diameter (m)
SOI	Start of Injection
SPJ	Single Phase Jet

List of Symbols

Latin Characters

c	passive scalar ($0 \leq c \leq 1$) or the liquid fuel to gas volume fraction
d	particle diameter (m)
f_i	i component of spray momentum source term
$\mathbf{f}$	the spray momentum source term
i	the imaginary unit ($i = \sqrt{-1}$)
$\mathbf{k}$	wave vector (1/m)
p	pressure (N/m^2)
$\mathbf{r}$	position vector
u_i	i component of velocity (m/s)
$\mathbf{u}$	velocity vector (m/s)
$\hat{\mathbf{u}}_\mathbf{k}$	the Fourier coefficient of the $\mathbf{k}^{th}$ mode of the velocity
C_D	particle drag coefficient
D	diameter, inlet diameter of the PLJ in the model problem (m)
D_{SM}	Sauter mean diameter (m)
L	integral length scale
Ma	Mach number
Oh	Ohnesorge number of a droplet, $Oh = \mu/\sqrt{\rho_d \sigma d}$
Re	Reynolds number, $Re = U\delta/\nu$
$\mathbf{S}$	The symmetric part of the velocity gradient tensor
St_p	Stokes number for a particle/droplet
T	temperature (K)
U	velocity, characteristic velocity (m/s)
U_o	jet inlet gas velocity (m/s)
V_f	in a multiphase flow the carrier fluid phase volume fraction
V_g	in a multiphase flow the gaseous phase volume fraction (same as V_f)
V_p	in a multiphase flow the particle phase volume fraction
We	Weber number of a droplet, $We = \rho_d \lvert U_p - U_g \rvert^2 d/\sigma$
D/Dt	the material derivative

Greek Characters

δ	characteristic length
δ_{ij}	Kronecker symbol
ϕ	the equivalence ratio
φ	mass loading ratio (*mass of injected fuel*/*mass of injected gas*)
ν	kinematic viscosity (m^2/s)
ρ	density (kg/m^3)
σ	surface tension
τ_p	particle momentum relaxation time (s)
τ_η	Kolmogorov time scale (s)
τ_f	integral time scale (s)
η	Kolmogorov length scale (m)
Λ_2	The second largest eigenvalue of the symmetric tensor $\mathbf{S^2 + \Omega^2}$
$\mathbf{\Omega}$	The antisymmetric part of the velocity gradient tensor

Subscripts

c	characteristic
f	fuel/fluid
g	gas
inj	injection
p	particle/droplet
t	turbulent

List of Figures

List of Tables

1 Introduction

1.1 Scope

The thesis consists of a brief introduction to the research field and discussion of the main results. The results are reported in the Publications I-VII that are attached to the end of the thesis. As the Publications contain much details on the simulations, this summary avoids repeating those details for brevity. Chapter 1 gives a rather general introduction to the research field and the research problem. Chapter 2 introduces the reader to the governing equations and certain theoretical concepts that the Author has found especially useful in understanding the research field. Chapter 3 presents the main findings of the thesis in light of previous studies. Chapter 4 gives a brief summary of the main results. In Chapter 5 a synopsis of the thesis is given. Finally, in Chapter 6 the conclusions are made and an outlook to future studies is given.

1.2 Background and Motivation for Fuel Spray Research

One of the driving factors in the development of diesel engines is the reduction of particulate matter and NOx emissions which are formed inside the combustion chamber during combustion. The level of *fuel-air mixing*, i.e. the *relative fuel to air ratio* or the *equivalence ratio* ($\phi = \phi(x, y, z, t)$), influences the actual combustion characteristics and the related chemical reactions. Soot formation is typically associated with fuel-rich regions of the combustion which occur in the vicinity of the *diesel spray* whereas NOx formation is related to the high temperature regions of combustion [1]-[3].

A famous result produced by Akihama et al. [4] using zero-dimensional detailed chemical kinetic model is shown in Figure 1.1. The result, i.e. a $\phi - T$ map, concerns the emissions that are formed when n-heptane burns. Figure 1.1 shows that the soot formation depends strongly on ϕ and that NOx formation depends strongly on the temperature ($T = T(x, y, z, t)$) at which the combustion takes place. As can be seen, the soot emissions decrease to nearly negligible values if $\phi < 2$. In practice, soot emissions are related to small sub-micrometer particles that may penetrate into human lungs and brains causing health problems. Hence, it is often desirable to optimize diesel engines in such a way that fuel consumption is minimized while meeting mandated emission levels. Thereby, new combustion concepts such as the Homogenous Charge Compression Ignition (HCCI) engine have been and are developed to keep the combustion conditions in the gray Low Temperature Combustion (LTC) area as seen in the Figure 1.1. It is a challenge to design such combustion conditions where low NOx and soot emissions could be achieved simultaneously since high NOx emissions are typically associated with low soot emissions and vice versa.

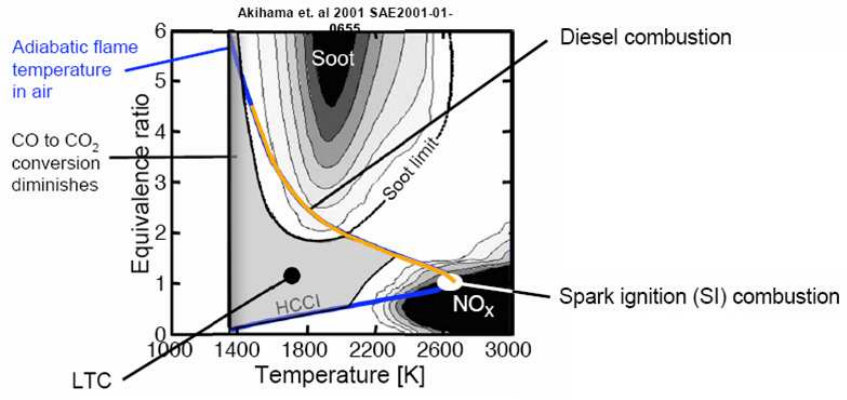

Figure 1.1: Soot-NOx emission diagram by Akihama et al. [4].

There are many parameters to consider in achieving the mandated emission levels. However, the fuel injection system is of primary importance since high injection pressures lead to enhanced atomization of the spray into small droplets which enhances the mixture formation. In specific, the effect of nozzle hole diameter is very

important since the decrease of the diameter has been noted to reduce the soot emissions [6]. The trends of increasing injection pressures and, thereby, decreasing droplet sizes in commercially available diesel engines are shown in Figure 1.2. Thus, the diesel fuel spray injection systems are under constant development and, although the field itself stems back to the invention of the diesel engine, it has turned out that the spray processes are still rather inadequately understood as implied in the review by Smallwood and Gülder [7]. Understanding the details of emission formation requires deeper understanding of the *physics of fuel sprays* and investigations on how a *fuel spray* cloud evolves and mixes [2].

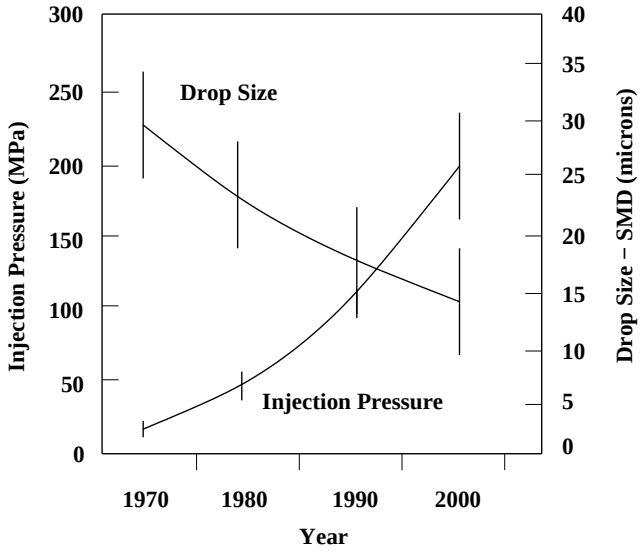

Figure 1.2: The rapid change in diesel engine technology has resulted in dramatically higher injection pressures and a related decrease in the mean droplet diameters. The bars represent the range found in commercially available diesel engines. (Reconstructed from the study by Smallwood and Gülder [7].)

1.3 Diesel Sprays

Overview: In diesel engines the fuel is injected into the cylinder by a high pressure atomizer with nozzle hole diameter d_n which creates the fuel spray. Investigations

on the spray formation process have a long history (e.g. [9, 55]). However, during the past decades the operation conditions of the diesel fuel injection systems have experienced a tremendous change and the most recent updates to the previously existing views have been reviewed by Smallwood and Gülder [7]. In contrast to spark-ignited engines, the diesel spray evaporates and ignites due to the increase of temperature during the compression stroke. A very useful first stage of understanding the fuel spray formation process is to study fuel injection and spray dynamics in non-evaporating and non-reacting conditions i.e. fuel injection at rather low temperatures. A diesel fuel spray under such conditions is seen in Figure 1.3. The Figure immediately shows that the boundary of the spray has irregular features which are due to *random motions* of the surrounding gas. These motions are further complicated by the presence of droplets. The spray has also a complex internal structure which is also random in character due to the motions of the gas. This random motion of gases and liquids, or, in brief *fluids*, is called *turbulence*. In contrast to smooth and slowly varying *laminar flows*, turbulent flows can be characterized by significant and irregular variation of fluid velocity in both space and time [8]. It is seen in Figure 1.3 that diesel sprays are typically cone-shaped and they have an opening angle α [1]. Furthermore, in contrast to *monodisperse* sprays where all droplets/particles are of the same size, the diesel spray is a *polydisperse* spray i.e. it is characterized by a *size distribution* of droplets [9]. Much of the conventional diesel spray research is related to investigations at non-evaporating and non-reactive conditions (e.g. [1, 5, 7, 11, 12, 17, 18]).

Deeper Look to the Effect of Nozzle Diameter on Soot Emissions: It is generally believed that small d_n implies improved mixing and decrease of soot emissions within the spray. However, there might be several reasons for this. In the context of conventional diesel sprays the connection between d_n and the flame lift-off lenght (i.e. the distance at which the flame starts from an injector) has been much emphasized lately as the investigations by e.g. Siebers and Higgins [5] as well as Pickett and Siebers [6] imply that air entrainment into the spray may be

enhanced with respect to the spray mass when d_n decreases. This might positively influence the air content within the fuel spray due to entrainment of fresh air during combustion. From the basic spray literature one may find also other supporting explanations to the decrease of soot emissions with d_n as discussed in what follows. Consider a cone-shaped spray with the injector as the 'sharp tip'. The cone angle is (α), the height of the cone increases due to to the spray tip penetration $(S = S(t))$ and thus also the bottom area of the cone at the tip location $(A = A(t))$ increases as $A \sim (tan(\alpha/2)S)^2$. Assume then that the well known correlation formulae $S \sim (td_n)^{1/2}$ and $tan(\alpha/2) \sim (\rho_g/\rho_f)^{1/2}$ hold for high pressure diesel injection so that α depends only on L_n/d_n ratio of the nozzle [1]. Furthermore, assume that the total injected spray mass $m_s \sim td_n^2$ at a constant injection rate as predicted by the Bernoulli equation [1]. Under these assumptions the volume of the spray is given by $V_s(t) = 1/3A(t)S(t)$ and hence the average fuel concentration (c_{ave}) inside the spray is given by $c_{ave} = m_s/V_s \sim (d_n/t)^{1/2}$. Hence, the literature suggests that small d_n, not only implies higher air entrainment, but also lower average concentrations inside the spray which should further reduce the soot emissions.

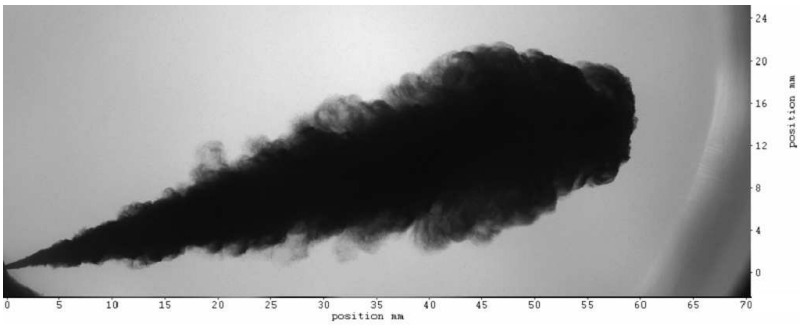

Figure 1.3: A shadowgraph visualization of diesel spray injection. The liquid fuel is injected via a high pressure nozzle which *atomizes* the fuel into droplets that form the turbulent spray cloud. Courtesy of Harri Hillamo (2008).

Diesel Spray as a Multiphase Flow: Turbulence is in a key role in the dynamics of *multiphase flows* such as dust/smoke clouds or rain showers [53, 54]. Fuel sprays in various combustion applications are also good examples of *particle- or droplet-*

laden flows. In diesel engines the fuel spray forms the point where, in addition to production of energy, a complex chain of events begin that determine the efficiency and emissions for a given engine [1, 2, 10]. Thus, there exists a continuous interest in understanding the spray processes in detail by experimental approaches [11]-[18], numerical simulations [25, 36, 46] and theoretical studies [55]-[65]. Also droplet level details including atomization and evaporation [9, 10, 55],[58]-[68] as well as turbulence modulation [70]-[76] and formation of dispersions [40]-[80] have raised a lot of interest.

1.4 Turbulence and Simulation

Description of Turbulence by the Navier-Stokes Equation: In 1822 *Isaac Newton's* second law of conservation of momentum was applied to the motion of fluids by *Claude-Louis Navier* and *George Stokes*. Their result is known today as the Navier-Stokes (NS) equation which is a partial differential equation that is believed to describe the *laminar* and *turbulent* motion of fluids accurately in the continuum limit i.e. above length scales that are much above the mean free path of a molecule. An essential feature of turbulent flows, in comparison to laminar flows, is that the fluid velocity varies significantly and irregularly both in space and time. The ability of turbulent flows to effectively mix entrained fluids to a molecular scale is a vital part of such flows and of vital importance and consequences in nature and engineering [96]. It has been suggested that turbulent mixing could be viewed as a three stage process of entrainment, dispersion (or stirring) and diffusion, spanning the full temporal and spatial spectrum of scales of the flow (see [96] and the citations therein).

Multiscale Nature of Turbulence: The Navier-Stokes equation describes the dynamics of tremendous contrasts due to the *multiscale nature of turbulence*. In fact, to date, analytical solutions to the three-dimensional NS-equation have not

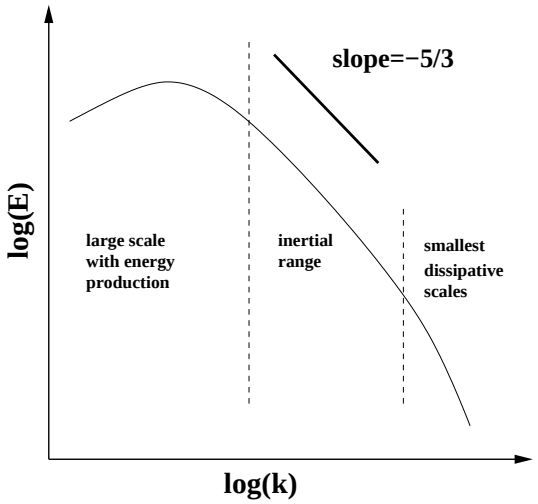

Figure 1.4: Kinetic energy spectrum of turbulence. Most of the energy is produced at the low wave numbers and dissipated at the highest wavenumbers. The wave number $k \propto$ inverse of length scale.

been found despite a few special cases in the laminar flow regime [8]. A useful way of understanding the time and length scales of turbulence is to consider the L-periodic *Fourier* composition of the velocity distribution $\mathbf{u}(x, y, z, t) = (u_1, u_2, u_3)$. The Fourier series for the velocity can be written as $\mathbf{u}(x, y, z, t) = \Sigma_{\mathbf{k}} \hat{\mathbf{u}}_{\mathbf{k}}(t) exp(-i\mathbf{k} \cdot \mathbf{r})$ [8]. The large scale motions (represented by the lowest wave-numbers) are affected by e.g. the boundary and the initial conditions, whereas the smallest turbulent scales (represented by high wave-numbers) depend mostly on the rate at which they receive energy from the largest scales. Thus, a turbulent flow can be viewed as a system where a *scale separation* between the large and the small scales of the flow exists: thin filaments of intense vorticity (small and chaotic eddies) are embedded in a background of weak vorticity (large and smooth eddies) [19]-[21]. In the final period of decay the smallest eddies disappear exponentially in time due to viscosity [8]. The 'flow' of energy from the largest integral scale L to the smallest scale η (the *Kolmogorov* scale) is the turbulent energy cascade as reflected to the individual wavelengths in the coefficients $\hat{\mathbf{u}}_{\mathbf{k}}(t)$. According to the *Kolmogorov* theory of homogeneous, isotropic turbulence, at a sufficiently high Reynolds number, there

is an intermediate range of scales where production of turbulence equals its viscous dissipation resulting in a famous $-5/3$ slope [8, 22]. Figure 1.4 shows a sketch of the spectrum of turbulent kinetic energy.

Computational Fluid Dynamics: CFD is the branch of science that considers the numerical simulation and modeling of fluid flows. The field has experienced a tremendous growth during the recent two decades due to the rapid growth of computer power although some of the used methods were developed and tested already by *John von Neumann* and his contemporaries [23]. In CFD a set of partial differential equations (PDE's), for example the *Poisson* or the Navier-Stokes equation, are discretized and solved on a finite number of grid points which describe the geometry and boundary conditions of the flow. From the engineering viewpoint the most common framework to do this is the finite-volume method (FVM) where the domain is divided into small 'control' volumes (tetrahedra, hexahedra etc). The governing equations are integrated over the control volumes, the non-linear terms are linearized and after this the *Gauss divergence theorem* is applied in order to transform volume integrals into surface integrals, or in physical terms, *fluxes*. The spatial coupling information between adjacent control volumes arises from the numerical evaluation of the fluxes (e.g. mass, momentum and energy) passing from one control volume to another. Various numerical techniques to solving the governing PDE's have been and are constantly developed [22, 23].

1.5 Complex Phenomena in Multiphase Flows

Particle-Turbulence Interactions: According to Elghobashi [81], the presence of a very wide spectrum of important time and length scales makes DNS of multiphase flows typically impossible. This, together with incomplete understanding of plain single phase turbulence, sets the upper limit to our current understanding of complex particle-laden turbulent flows [81]. However, despite the difficulties, there are many

things that can be said about such flows. For example, it is clear that particles and the carrier phase interact with one another. According to the characterization by Hinze (see [10] and the citations therein) several turbulence modification mechanisms may be identified. Two of these mechanisms are of particular interest: 1) exchange of kinetic energy between a particle and an eddy as the particle accomodates to the eddy velocity (turbulence modulation) and 2) the direct disturbance of the continuous-phase velocity field by particle wakes (turbulence generation). Crowe notes that several sources of turbulence in the carrier phase due to particles have been identified [72]. These include 1) streamline distortion due to the presence of particles, 2) the wake generated by the particles, and 3) the modification of the velocity gradients in the carrier phase and the associated change in turbulence generation and the damping of turbulence motion by the drag force on the particles. The wake generated by large particles has been related to droplet Reynolds number Re_p and the analysis has implied that when $Re_p > 300$ the unsteady particle wake may interact with the turbulent scales [61]. However, in diesel sprays it is desirable to atomize the droplets into small enough fragments so that in modern engines $Re_p < 300$. Hence, the wake induced turbulence production is not likely to be process governing phenomenon in diesel sprays.

One-, Two- and Four-Way Coupling: In homogeneous turbulence, the momentum coupling between particles and the carrier phase has been characterized by Elghobashi [82] in which one has divided the different regimes of particle-carrier-flow interactions into one-, two- and four-way coupling as a function of particle to fluid volume fraction

$$c = V_p/V_f \tag{1.1}$$

and the particle Stokes number St_p which is defined as

$$St_p = \tau_p/\tau_f. \tag{1.2}$$

Here the particle momentum relaxation time is the timescale at which a particle accomodates to the local flow conditions (e.g. stops in a quiescent fluid) and it is

defined as

$$\tau_p = \frac{\rho_p d^2}{18\rho_g \nu} \tag{1.3}$$

and τ_f is the characteristic time of the fluid phase. For example, in this work τ_f is defined as

$$\tau_f = D/U_o, \tag{1.4}$$

where the jet diameter ($D = 0.002m$) is used as a measure for the integral length scale and gas jet velocity at inlet ($U_o = 80m/s$) as the integral velocity. If two- and four-way coupling are considered, particles with $St >> 1$ may *produce* turbulence whereas particles with $St << 1$ may *dissipate* turbulence. In fact, the strength of the coupling should also be dependent on the particle to gas *mass-loading*. More aspects on the turbulence modulation effects have been discussed in the literature [53, 54].

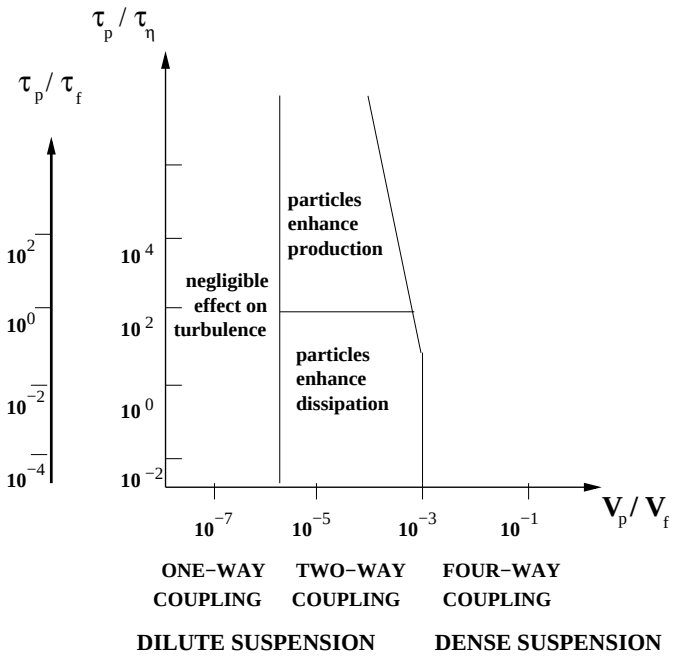

Figure 1.5: Coupling regimes between particles and carrier phase (reconstructed from [82]). Here V_p/V_f is the particle to fluid volume fraction.

Figure 1.5 characterizes the different regimes of particle-gas phase coupling [82]. The given characterization by Elghobashi [82] may be applied to fuel sprays as follows. Assuming a cone-shaped spray with opening angle α, it is straightforward to estimate that in diesel sprays four-way coupling is expected to take place at least when $\left(\frac{d_{inj}/2}{tan(\alpha/2)z}\right)^2 > 10^{-3}$ i.e. until volume fractions are lower than 10^{-3} when two-way coupling is dominating and four-way coupling is less important. This estimate translates to distances $z < 150 d_{inj}$ from the nozzle exit depending on void volume fractions at the nozzle which may be affected by e.g. cavitation effects [1, 25].

1.6 Simulation of Turbulence and Particle Laden Flows

RANS, LES and DNS: In turbulent flows a wide range of length and time scales are present. Because of the computational limitations of the present-day computers, these scales can not be fully resolved for technically relevant flows and hence the turbulent motions need to be modeled. The purpose of *turbulence models* is to emulate the motion of the smallest scales which enables computer simulations on reasonably coarse computational grids and reasonable time-step sizes. The turbulence modeling approach depends much on the physical system that is to be studied (e.g. geometry and dimensions) and on the desired level of information. The conventional way of simulating turbulent flows is the Reynolds Averaged Navier-Stokes (RANS) approach where turbulence is modeled and the average motions are solved [8]. This means that the unsteadiness is modeled with a turbulence model that increases the viscous dissipation. The RANS framework is derived by time-filtering the Navier-Stokes equations. Hence, by definition, RANS provides time-averaged information of the flow field. RANS is especially suitable for large scale industrial simulations and has been applied in many other applications as well including internal combustion engine simulations [25, 26]. The more advanced turbulence simulation approach that is becoming more and more popular is the Large-Eddy Simulation (LES) framework where only the subgrid scale (SGS) turbulence is modeled as enhanced dissipation

and the unsteady motions at the grid scale are explicitly solved. The LES framework can be formally derived by spatially filtering the Navier-Stokes equations which leads to the same equations in terms of the filtered variables and new SGS-terms that can not be expressed in terms of the filtered variables due to the non-linearity of the convection term [8]. Hence, the SGS-terms need to be either explicitly modeled with a SGS-model or implicitly modeled with a dissipative numerical scheme. LES is a step towards Direct Numerical Simulation (DNS) where the whole turbulence spectrum is solved on a very fine grid [8, 22, 23].

Implicit LES: A method in between LES and DNS is so called *implicit* Large-Eddy Simulation (ILES) which is also the method applied in this work in Publications II-VII. Recently there has even been a text book published on the topic [46]. Thus, ILES approach has become more and more popular in the literature and it is based on the idea of carrying out the simulations on a fine grid and then using a dissipative numerical scheme in order to stabilize the computation. In fact, the idea was applied already by von Neumann in the 1950s to stabilize finite-difference computations related to shock wave propagation [20, 23]. Many authors have used ILES in the context of wall-bounded flows [19]-[21],[46, 47], free-shear flows [48, 50], and the combination of these two [49]. Prior to the present work, ILES has also been applied to compressible flows [46, 50] and to the simulation of sprays [47, 51, 52]. In general, the simulation of turbulent flows is a very delicate task and hence not all implicit LES will work. Some of the pre-requisities for ILES are: 1) a fine enough grid so that the Taylor microscale is properly captured [48, 49], 2) adequate temporal accuracy to resolve the highest temporal frequencies, 3) the numerical algorithm has to be not too dissipative, yet, dissipative enough so that the turbulent energy cascade does not accumulate energy at the highest wave numbers [46], and 4) the numerical method should not 'contaminate' the large scale features of the flow [8, 46]. Further discussion on the advantages and disadvantages of ILES has been given by Pope [8].

RANS-Modeling of Sprays: During the past 2-3 decades, spray simulations have

been carried out with RANS turbulence models [25]. In specific, in the context of RANS-modeling, the role of the KIVA-code, developed at the *Los Alamos National Laboratories*, should be mentioned [26]. The family of KIVA-codes are one of the basic platforms where many CFD-submodels related to sprays and combustion have been developed for the purposes of the automotive industry and the academia (see e.g. [24]-[29]).

LES-Modeling of Sprays: LES has become more and more popular during the past ten years but it has not yet replaced RANS as LES typically requires much finer spatial and temporal resolution in comparison to RANS. Hence, efficient parallelization is required in order to achieve reasonable run times. In this work, for example, 1000-3000 CPU hours was considered to be 'reasonable' since parallelization onto 32 processors yielded a simulation to take only 2-4 days. Quite recently, LES has been implemented to the KIVA-code as well. For example, Hori et al. [30] implemented the k-equation turbulence model to the KIVA code and showed by direct comparison between LES and RANS approaches that, unlike RANS, LES is capable of producing the transient features of sprays including the small scale (i.e. grid scale) vortex structures. Examples on the use of LES in large scale parallel simulations on particle laden jets with a range of droplet sizes are those by Apte et al. [31, 32], Ham et al. [33], Menon et al. [34] and Pitsch et al. [35]. These studies concern realistic industrial combustors where droplets are injected into a co-annular jet. By comparison of the results with experimental data, it is shown that the LES approach can produce realistic information on droplet dispersion and the consequent evaporation statistics. LES also produces the large scale flow structures including the ring vortices that are formed around the circular jets [31, 36]. Recently, Oefelein et al. [37] and Bini and Jones [38] have applied LES to study evaporating sprays in various conditions.

DNS of Sprays: There have also been DNS studies on particle laden free shear flows using DNS in the one-way coupling regime. For example, the effect of St_p on

mixing has been investigated in a three-dimensional particle laden mixing layer by Ling et al. [40]. Luo et al. studied the dispersion of round particles in a plane jet at $Re = 3000$ [40]. Recently, similar studies on plane jets have been carried out by Yan et al. [42]. The previous LES and DNS studies support the transition towards these methods because LES provides a more detailed temporal and spatial picture of mixing (see sections 2 and 3 for further discussion).

1.7 Research Problem

1.7.1 Framing of the Problem

The 'Real World' Problem: The behavior of the combustion in a diesel engine strongly depends on the spray distribution prior to ignition [10, 97]. The heterogenous nature of mixing has been related to droplet size and strong internal heterogeneities in spray structures have been clearly demonstrated by experiments (c.f. [12, 18]). A highly interesting engine concept is the HCCI-engine in which the particulate and the NOx emissions could be substantially reduced [4]. As the fuel injection in such an engine typically takes place at low temperature conditions, the spray evaporation during the injection is not the process determining step as in a conventional diesel engine. Also, when far enough from an injector, the droplet breakup has become less important. Thus, in such a situation, the understanding of spray formation including the interplay between the fuel droplets and the turbulent gas is highly relevant because these interactions determine the mixture quality and thereby they affect the emission levels. These interactions can be studied with the particle-laden jet model problem as explained in the text below.

Methods and the Model Problem: Diesel spray research is a multi-disciplinary field with experimental, computational and theoretical components. The present

research deals with the physics of fuel sprays. Numerical simulations and modeling are used to investigate fuel spray formation and mixing. The simulation methods are based on applied mathematics and principles of computational fluid dynamics. In addition, concepts from turbulence theory, statistical mechanics and liquid atomization are used. The research problem stems from the need to understand and simulate fuel sprays in a more accurate and realistic manner. As implicit Large-Eddy Simulation (ILES) is known to capture transient features such as small scale eddies of turbulent flows, it is expected that ILES and Lagrangian Particle Tracking (LPT) together are suitable methods for capturing the structure and transient nature of sprays as well. In order to emulate a spray a choice was made to study a model problem of a droplet-laden i.e. a particle-laden jet (PLJ) which avoids the inconsistencies of LES/LPT approach near the injector

The Key Physical Phenomena: The primary physical phenomenon that is studied in this work is *dispersion* of droplets by turbulence. Turbulent flows have a certain mixing potential that causes droplets to disperse and hence this phenomenon and especially the effect of St_p on the strength of the phenomenon is to be studied. The secondary physical phenomenon of interest is droplet breakup because droplet breakup reduces St_p and thereby the active presence of the phenomenon is expected to enhance dispersion. A choice was made not to model other spray phenomena such as evaporation or combustion.

1.7.2 The Computational Setup

Illustration of the Setup: In Publications II-IV the studied computational case setup is the same. In Publications V-VII the setup is improved from the viewpoint of mesh resolution and time integration method. The details are explained in the Publications and the studied cases are summarized in section 4.2. Here the basic setup, as depicted in Figure 1.6, consists of a gaseous laminar *jet* with 'top-hat'

velocity profile that exits from a round hole into a vessel of quiescent gas. In the vessel the jet can freely spread. The jet is randomly *seeded* with droplets that form the droplet dispersion i.e. the spray cloud. Hence, the gaseous jet forms the *base flow* in which the cloud formation may be studied. From the literature, it is expected that the chosen base flow is suitable for studying spray formation [42, 43]. The Reynolds number of the base flow is $Re = 10^4$ and the Mach number is $Ma = 0.3$. Much of this thesis concerns explaining what is seen in the Figure 1.6. In fact, the physics of the situation has many things in common with smoke that exits from a chimney.

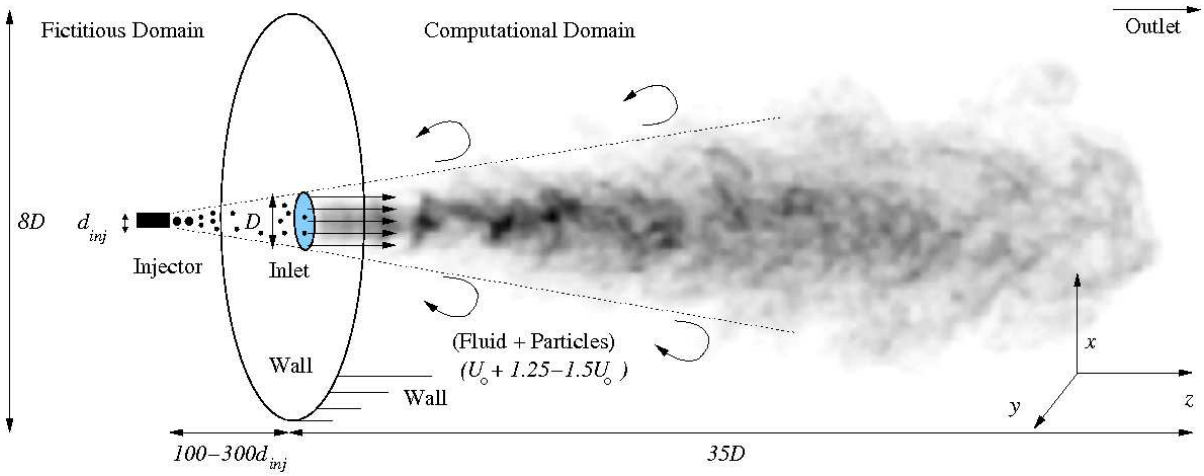

Figure 1.6: A particle laden jet that contains small particles. As can be seen, Large-Eddy Simulation captures the random, coherent structures of the jet which can be seen by looking at the boundary of the cloud. The average velocity of the incoming stream is $U_o = 80m/s$ and the velocity has a top-hat profile. The velocity of the particles is varied and it is higher than the gas velocity. Much of this thesis concerns explaining what is seen in this Figure.

The Key Parameters of the Model: In all the cases the velocity of the incoming gas stream is $U_o = 80m/s$ that is randomly perturbed. The droplet velocity is varied between $1.25 - 1.5U_o$ to emulate the two-way coupling. A higher value of initial slip velocity has a stronger effect to the properties of the base flow and hence a rather

low value for initial slip was chosen to ease the analysis. The main parameter that is varied in the simulations is the droplet diameter (d). Also the amount of the injected spray mass has been varied in the simulations. This can be expressed as the mass loading ratio (φ):

$$\varphi = \frac{mass\ of\ injected\ fuel}{mass\ of\ injected\ gas}. \tag{1.5}$$

Also the spray opening angle could be varied but a decision was made to set it to zero in which case the dispersion is fully due to turbulent fluctuations as produced by the shear layer. The fluid timescale τ_f is defined by using the integral time scale:

$$\tau_f = T = D/U_o, \tag{1.6}$$

which is referred to the jet inlet diameter D and velocity U_o. The integral timescale describes the large eddy turn-around time and the period of oscillation for the lowest characteristic frequencies of the fluid phase. The droplet timescale is defined as

$$\tau_p = \frac{\rho_p d^2}{18\rho_g \nu_g} \tag{1.7}$$

and it is the measure of deceleration/acceleration periods of droplets in turbulent fields [1, 25].

1.7.3 The Research Question and the Objectives

Research Question: The study aims to bring insight to the following research question: *How can droplet size originated differences in spray shapes be measured, quantified or statistically analyzed and what is the connection between spray shape and mixing?*

Objectives: The main objectives of the thesis are listed below:

- A model problem of a spray, a droplet laden jet, is to be investigated to understand the role of droplet size to mixture formation.

- The spray cloud shape is to be visualized in a realistic manner as seen in experiments and, in specific, previous numerical works on particle laden flows.
- Visual information should be combined with clarifying statistical measures that explain the effect of droplet size on spray cloud formation.

1.7.4 Simulations and Computational Tools

The main computational tool used in this work is the OpenFOAM open source code that is written in the C++ language. OpenFOAM applies for parallel computing and the code is provided with several CFD-solvers [83]. In this work two of the standard existing solvers called *Xoodles* and *dieselFoam*, were combined to create a spray solver which is capable for both low and high Mach number spray simulations [83]-[85]. This solver was then used to execute a series of test runs of which each used about $1500-2000$CPU hours of computation time at the CSC supercomputers. Altogether approximately 70 runs were carried out of which about 40 are reported herein. Hence, approximately 100000CPU hours of computational resources were used during this work. Each of the runs produced ca 10GB of data which was post-processed with *Matlab*. In Publication II also the *Paraview* program was used for data visualization. The post-processing and the data that was analyzed and printed out from the simulations was much improved during this work and in the final stage all the analysis was carried out with *Matlab*. More information on the code details and validation of the code are found in the literature [83, 86].

1.8 Main Contribution

The main focus in this thesis is to explore a target case common to Publications II-VII from different viewpoints. The main achievements, that were unclear topics

before this thesis, are listed below:

- In Publications II-VII the internal and external structure of simulated sprays has been visualized. Different mixing patterns have been observed as a function of droplet Stokes number.
- In Publications V-VII a novel spray visualization algorithm is developed which can be utilized as a post-processing tool to create spray images similar to experiments from the simulation data using the parcel coordinates.
- In Publications V and VII the mixing of droplets has been quantified in terms of mixing indices that depend on droplet size and arise due to turbulent fluctuations of the carrier phase. To the knowledge of V.Vuorinen this work is the first attempt to associate a quantitative measure with a spray shape.
- In Publications IV, V and VI statistical, droplet level analysis of the slip velocity probability distributions has been used. The analysis explains differences in the cloud shape.
- In Publication V a new droplet breakup model has been developed. The paper points out an issue that is often omitted in droplet breakup modeling: droplet breakup in a turbulent flow might be a rather different phenomenon from breakup in a laminar flow. The numerical experiments demonstrate that large differences in spray mixing can be potentially observed if the low Weber number breakup is modeled.

2 Governing Equations

2.1 The Filtering Effect of Diffusion

Turbulence Modeling in Brief: The numerical stability of RANS and LES turbulence modeling is based on artificial *smoothening* (i.e. *filtering*) of the numerical velocity field by a diffusive mechanism. This means that one defines an effective viscosity $\nu_{eff} = \nu + \nu_t$, where ν is the kinematic viscosity of the fluid and ν_t is the turbulent viscosity that is calculated in the turbulence model. In a standard situation, $\nu = const.$ and $\nu_t = \nu_t(x, y, z, t) \geq 0$ where the positive value of ν_t prevents the back-scatter of energy from the small scales to the large scales [8]. In the RANS framework ν_t is typically defined by using e.g. the turbulent kinetic energy and its dissipation rate. In the LES framework one may use e.g. the symmetric part of the velocity gradient tensor to find ν_t as is done in e.g. the Smagorinsky model. In ILES a somewhat dissipative numerical scheme is applied and $\nu_t = 0$. Hence, in ILES ν together with the truncation error of the numerical scheme cause the dissipation. In DNS all the scales of the flow are solved with a non-dissipative numerical scheme and thus ν alone dissipates the smallest eddies. In fact, the smallest scales of the flow decay exponentially in time as can be also seen in what follows [8].

A Fourier-Series Example: An illuminating example on the filtering effect of diffusion is given. A standard method of solving partial differential equations (PDE's) is to expand the solution in a series of orthogonal functions [87]. In Fourier analysis the function basis set is chosen to be the spatially oriented plane waves:

$$\phi_{\mathbf{k}}(x, y, z) = e^{i\mathbf{k}\cdot\mathbf{r}}, \tag{2.1}$$

where the wave-vector $\mathbf{k} = (\frac{2\pi l}{L}, \frac{2\pi m}{L}, \frac{2\pi n}{L})$ and the radial coordinate $\mathbf{r} = (x, y, z)$. Discrete and continous Fourier transforms are frequently applied in the theory and simulation of turbulence [8, 88]. In 3D, the Fourier series representation for a func-

tion $f = f(x, y, z)$ (that is assumed to be L^2-integrable and can be real or complex valued) reads:

$$f = \Sigma_{\mathbf{k}} \hat{f}_{\mathbf{k}} \phi_{\mathbf{k}}, \;\; \hat{f}_{\mathbf{k}} = (2\pi)^{-1}(f, \phi_{\mathbf{k}}). \tag{2.2}$$

The set of functions $\{\phi_{\mathbf{k}}\}$ is an orthogonal system over the cube Ω and the inner product $(.,.)$ is defined as

$$(f, g) = \int_{\Omega} f(x, y, z)\overline{g(x, y, z)} d\Omega. \tag{2.3}$$

Let us next demonstrate the effect of the Laplacian operator $\Delta = \Sigma \frac{\partial^2}{\partial x_i^2}$ on a numerical solution in Fourier-space. Consider the basic heat equation i.e. the diffusion equation for the temperature distribution $T = T(x, y, z, t)$ in the cube Ω [87]

$$\begin{cases} \frac{\partial T}{\partial t} = \nu \Delta T \\ T(x, y, z, t = 0) = g(x, y, z), \end{cases} \tag{2.4}$$

with periodic boundary conditions. In equation (2.4) ν is the heat diffusivity. The problem can be solved by separation of variables [87] with the Fourier series Ansatz $T = \Sigma_{\mathbf{k}} \hat{T}_{\mathbf{k}}(t) e^{i\mathbf{k}\cdot\mathbf{r}}$ yielding

$$T = \Sigma_{\mathbf{k}} \hat{T}_{\mathbf{k}}(0) G_{\mathbf{k}}(t) e^{i\mathbf{k}\cdot\mathbf{r}}, \tag{2.5}$$

where $G_{\mathbf{k}}(t) = e^{-|\mathbf{k}|^2 \nu t}$. The solution reveals that, starting from a given initial temperature distribution, during a small time interval Δt, the highest wave-number components are the most affected i.e. damped by the factor $G_{\mathbf{k}}(\Delta t) = e^{-|\mathbf{k}|^2 \nu \Delta t}$. In contrast, the low wave-number components are hardly affected as $G_{\mathbf{k}}(\Delta t)$ is of order unity for low $\mathbf{k}$. It can also be seen that only the zero'th mode $\hat{T}_0$ remains unaffected (it is multiplied by 1). This can be understood by means of conservation of internal energy since $\hat{T}_0$ corresponds to the mean temperature around which the temperature fluctuates. Eventually the temperature saturates to $\hat{T}_0$. If the high-frequency components of the solution are associated with those parts of the initial condition where high gradients exist, it can be stated that the small scale fluctuations in the initial condition vanish much faster in time than the global (large scale) features [88].

The discussion above points out the important effect of viscosity to different scales of the flow field and contains the essential information to understand what RANS and LES turbulence modeling as well as DNS is about. The given example shows that the effect of diffusion, as realized by the Laplacian operator in the physical space, is to *dampen* the Fourier modes in the spectral space. In the example above the effect of diffusive dampening is of *global* nature because it affects all the Fourier components. In contrast, the dampening could also take place via a *local* mechanism as is done when $\nu_t = \nu_t(x, y, z, t)$ [8, 88].

2.2 Introduction to the Navier-Stokes Equation

2.2.1 Convection-Diffusion Equation

Consider any conserved (real valued) physical quantity $c = c(x, y, z, t)$ that varies in space and time due to molecular diffusion and a moving carrier phase. For example, c could represent the concentration of milk when poured into a cup of coffee at constant fluid temperatures. The carrier phase velocity is given by a vector valued function $\mathbf{u} = \mathbf{u}(x, y, z, t)$ and the characteristic molecular diffusion constant of the species c is ν_c. The dynamics of c can be described with the general transport equation, the *convection-diffusion equation*, for a conserved scalar quantity [8, 22]:

$$\frac{\partial c}{\partial t} + \nabla \cdot (c\mathbf{u}) = \nabla \cdot \nu_c \nabla c. \tag{2.6}$$

In equation (2.6) the first term represents the (Eulerian) temporal partial derivative at a fixed position i.e. how c changes in time at the point (x, y, z). The second term implies that c is convected at the presence of a velocity field $\mathbf{u}$ and the last term represents the molecular diffusion. In comparison to convection, diffusion is typically a very slow process that is realized by molecular viscosity at small length scales. This effect was seen in the previous section from the Fourier series solution for the heat diffusion equation (2.5) which showed that, during small times, the

large scale (low wave number) components of the solution are hardly affected by diffusion.

2.2.2 Navier-Stokes Equation

The incompressible Navier-Stokes equations describe the flow of an incompressible Newtonian fluid [8, 22] (e.g. water) and gases (e.g. air) at low Mach numbers ($Ma < 0.3$) [22, 23, 88]. The Navier-Stokes equations, for a constant density fluid ($\rho = const.$) are:

$$\frac{\partial u_i}{\partial t} + \frac{\partial (u_i u_j)}{\partial x_j} = -\frac{1}{\rho}\frac{\partial p}{\partial x_i} + \nu \Delta u_i + f_i \tag{2.7}$$

$$\frac{\partial u_i}{\partial x_i} = 0, \tag{2.8}$$

where the unknowns are the components of the velocity field $\mathbf{u} = (u_1, u_2, u_3)$ and the pressure field p. In the equations above, the *Einstein* summation convention is applied so that summation is carried out over indices that appear twice. In the spray application the momentum source $f_i = f_i(x, y, z, t)$ corresponds to the droplet-originated momentum at a given position.

2.2.3 Large-Eddy Simulation

In LES the Navier-Stokes Eqs. (2.7)-(2.8) (or their compressible form as in Publications II-VII) are spatially filtered assuming that the filtering operator is commutative with the differential operator [8]. The filtering of the linear terms leads to the same terms for the filtered variables. In contrast, the filtering of the non-linear terms leads to a similar term with the filtered variables with additional sub-grid scale (SGS) terms. These terms cannot be expressed in terms of the filtered variables due to the non-linearity of the governing equations [8, 20]. When the resolution of the simulation is fine enough (i.e. capturing very large portion of the kinetic energy of

the turbulent fluctuations) the SGS-terms have only minor contribution and therefore they can be neglected altogether since the role of the SGS terms is to account for the interaction between the resolved and the unresolved scales. Dissipation of turbulent energy takes place at the smallest (Kolmogorov) scales [8, 46]. Thus, the role of the SGS term has to be accounted for explicitly (e.g. by an explicit SGS model) or implicitly (e.g. through a numerical scheme). In implicit LES this means that Equations (2.7)-(2.8) are numerically solved for the filtered variables and the SGS terms are neglected. In our calculations the resolution and the numerical dissipation have been found to be adequate to resolve a range of frequencies so that the large scale motions are adequately captured.

2.2.4 Pressure Equation

Taking the divergence of the Equation (2.7) and using the incompressibility constraint $\nabla \cdot \mathbf{u} = 0$ one obtains the Poisson equation for the pressure:

$$\Delta p = -\rho \frac{\partial u_i}{\partial x_j} \frac{\partial u_j}{\partial x_i} + \frac{\partial f_i}{\partial x_i} \tag{2.9}$$

which enforces the conservation of mass. The role of pressure in the NS-equation may be understood from the viewpoint of a so-called *Helmholtz-Hodge* decomposition of vector fields [88]. The Helmholtz-Hodge decomposition forms the theoretical basis for pressure correction methods (e.g. the PISO method) and the theorem states that any vector field $\mathbf{u}^*$ may be expressed as

$$\mathbf{u}^* = \mathbf{u} + \nabla q, \tag{2.10}$$

i.e. as a sum of a divergence free field $\mathbf{u}$ and a gradient of a scalar field $q = q(x, y, z)$. Due to the *elliptic* nature of the Poisson equation, small pointwise changes in velocity gradients are immediately reflected everywhere in the flow field [87]. Hence, although of little practical significance, in incompressible flows the pressure may be formally expressed in integral form by convoluting the right hand side of

equation (2.9) with the fundamental solution of the Poisson equation (the *Green* function) [8]. However, in practice (i.e. numerical applications), the solution of the pressure equation requires the solution of a linear system of equations [22].

2.2.5 Modeling the Motion of Particles and Droplets

In LPT the momentum source $f_i = f_i(x, y, z, t)$ $(i = 1, 2, 3)$ is constructed from a discrete field of point particles. The motion of the droplet parcels is governed by Newton's equation of motion [1, 26, 100]. It is assumed that the force acting on a droplet is due to the drag (with the coefficient C_D). The droplet (i.e. parcel) equation of motion reads

$$\frac{1}{6}\rho_p \pi d^3 \frac{d\mathbf{u}_p}{dt} = \frac{1}{2}(\mathbf{u}_g - \mathbf{u}_p)|\mathbf{u}_g - \mathbf{u}_p|\rho_g C_D \frac{\pi d^2}{4}, \tag{2.11}$$

where $\mathbf{u}_p$ is the particle velocity, $\mathbf{u}_g$ is the gas velocity that is interpolated to the particle position from the adjacent cells and C_D is the droplet drag coefficient. Eq. (2.11) can be cast into the following form

$$\frac{d\mathbf{u}_p}{dt} = \frac{C_D}{\tau_p}\frac{Re_p}{24}(\mathbf{u}_g - \mathbf{u}_p) \tag{2.12}$$

which is useful due to the explicit appearance of the droplet timescale τ_p given by Equation (1.7). The droplet Reynolds number is defined by

$$Re_p = \frac{|\mathbf{u}_g - \mathbf{u}_p|d}{\nu_g} \tag{2.13}$$

and the expression for the drag coefficient C_D is given by

$$C_D = \begin{cases} \frac{24}{Re_p}\left(1 + \frac{1}{6}Re_p^{2/3}\right) & Re_p < 1000 \\ 0.424 & Re_p \geq 1000. \end{cases} \tag{2.14}$$

An important non-dimensional number, i.e. the Stokes number (St_p), arises by non-dimensionalizing Eq. (2.12) with the integral timescale $T = D/U_o$:

$$St_p = \tau_p \frac{U_o}{D}. \tag{2.15}$$

In the proximal region of the jet the energy-containing frequencies are of the order $f \sim 1/T$ and hence referring St_p to the mean flow timescale $T = \tau_f$ is a good measure. It should be noted that the Eq. (2.11) is quadratic in terms of the slip velocity. This makes the coupling between the droplets and the gaseous phase non-linear.

The parcels are advanced in time using a semi-implicit time integration method by taking five sub-iterations within each time-step. The parcel position is updated through

$$\frac{d\mathbf{x}_p}{dt} = \mathbf{u}_p. \tag{2.16}$$

The instantaneous momentum source $\mathcal{M}(x, y, z, t)$ is evaluated for each cell separately by looping over all the parcels in a given cell, computing the lost momentum during the time-step by computing the velocity change from Eq. (2.12) and multiplying the acceleration by the parcel mass. During a time-step, it is also possible that a parcel moves from one cell to another. If this is the case the released/absorbed momentum is computed and shared between the cells accordingly (proportional to the time fraction the parcel spends in the associated cells inside the time-step). More details on the implementation of the LPT schemes and sub-models in the present code are described in [28, 29, 83].

The features of the present LES/LPT have been explained in detail in the Publications V-VII and these aspects are briefly summarized here. It is noted that in the present LES/LPT approach the grid can not be made much finer since this would be inconsistent with the assumption that the droplets do not displace the carrier fluid. Another issue associated with LES is the time-step size. With improved spatial resolution, smaller time-steps have to be used. Then, the minimum droplet relaxation time, τ_p, sets a restriction to the timestep length Δt in the droplet equations, which should be smaller than the smallest droplet momentum relaxation time. In the simulations $\Delta t \ll min(\tau_p)$ so that the droplet motion becomes resolved also for the smallest droplets. The inverse of τ_p is proportional to the change in the force

that the droplet motion has on the carrier phase. Thus, very small values of τ_p lead to large change in the right hand side of the momentum equations which may lead to numerical instability. For the large droplets having a large St_p the numerical stability problems are small since the cell-droplet momentum interaction is small as compared to the other terms in the momentum equations.

Good resolution LES implies that the sub-grid scale fluctuations are weak and hence those fluctuations can hardly modulate the motion of the droplets. If this is not the case, one may add the effects of the SGS fluctuation in a way similar to the one used in the RANS framework [25, 26]. Thus, from the SGS model, one may assess the magnitude of the SGS velocity fluctuation. Then, a random vector of length equal to the local SGS speed can be generated and then added to the resolved velocity when computing the acceleration of the droplet. Apte et al. [32] have pointed out two aspects regarding the effect of subgrid scales on the particles: 1) the effect of subgrid scales modeling is assumed to be important when there is a large amount of kinetic energy in the subgrid scales and when the SGS timescale is large in comparison to the characteristic droplet timescale, 2) if a SGS model is employed the particles do feel the effect of the subgrid scales by the resolved scale velocities. Examples of a LES/LPT where the effect of SGS fluctuations on the droplet motion is explicitly considered (by adding a random vector to the gas velocity at droplet position) are those by Oefelein et al. [37] and Bini and Jones [38]. This can be considered to be a consistent approach since an explicit SGS model was used in both studies. In this study, however, it is assumed that the effect of subgrid scales is altogether small and hence the motion of the droplets is simulated using the Eqs. (2.11)-(2.16) as such.

2.2.6 Spectral View of the Navier-Stokes Equation

It is very instructive to look at the NS-equation in the spectral space as this provides a deeper understanding on the structure of the equation and on the possible role of

the spray source term [8, 88]. For the moment, assume $f_i = 0$. In the theory and simulation of homogeneous turbulence the velocity and pressure fields are expanded in Fourier series

$$\mathbf{u}(\mathbf{r},t) = \Sigma_{\mathbf{k}}\hat{\mathbf{u}}_{\mathbf{k}}(t)exp(-i\mathbf{k}\cdot\mathbf{r}) \tag{2.17}$$

$$p(\mathbf{r},t) = \Sigma_{\mathbf{k}}\hat{p}_{\mathbf{k}}(t)exp(-i\mathbf{k}\cdot\mathbf{r}). \tag{2.18}$$

In Fourier space Eqs. (2.7) and (2.8) become

$$\Big(\frac{d}{dt} + \nu|\mathbf{k}|^2\Big)\hat{\mathbf{u}}_{\mathbf{k}}(t) = -i\mathbf{k}\hat{p}_k + \hat{\mathbf{c}}_k \tag{2.19}$$

$$i\mathbf{k}\cdot\hat{\mathbf{u}}_{\mathbf{k}} = 0, \tag{2.20}$$

where $\hat{\mathbf{c}}_{\mathbf{k}}$ is the Fourier coefficient of the $\mathbf{k}^{th}$ mode for the convection term $\frac{\partial u_i u_j}{\partial x_j}$. Eqs. (2.19) and (2.20) are a group of ordinary differential equations for the Fourier coefficients from which the pressure may be eliminated by dotting (2.19) with $\mathbf{k}$ and using (2.20). This yields

$$\Big(\frac{d}{dt} + \nu|\mathbf{k}|^2\Big)\hat{\mathbf{u}}_{\mathbf{k}}(t) = \hat{\mathbf{c}}_{\mathbf{k}} - \mathbf{k}\frac{\mathbf{k}\cdot\hat{\mathbf{c}}_{\mathbf{k}}}{|\mathbf{k}|^2}, \tag{2.21}$$

which is an ordinary differential equation [8, 88]. The RHS of Eq. (2.21) shows clearly how pressure acts as a projection operator on the non-linear term which 'keeps' each of the Fourier modes of velocity divergence-free [8].

Assume now the general case where the source term $f_i \neq 0$. The outcome of a multiphase CFD simulation depends much on Eq. (2.14). A minimum requirement is that the droplet timescale has to be captured by an LPT simulation i.e. $\Delta t < \tau_p$. However, as the Lagrangian particles are assumed to be subgrid scale in size, the LPT approach does not account for local (subgrid scale) spatial effects due to the motion of the particle wake. Hence, in Eq. (2.7), the spray source term could be understood in terms of the Fourier decomposition $f_i = \Sigma_{\mathbf{k}}\hat{f}_{i,\mathbf{k}}(t)exp(-i\mathbf{k}\cdot\mathbf{r})$ which may modulate the spatio-temporal properties of the carrier phase on the resolved time and length scales. However, as discussed by Mittal [61], if $Re_p > 300$ the motion of the unsteady wake produced by the particle might be important. For

example, it is possible that the wake behaves like an oscillator and returns large amounts of energy to the surrounding fluid in resonance. This phenomenon is not accounted for in LPT. Some of the particle Reynolds number effects are further considered in e.g. [10, 44, 75, 81]. In this work only particles with $Re_p < 300$ are considered which is often the case in modern diesel engines where fuel is atomized into very small droplets.

2.2.7 Numerical Solution of the Navier-Stokes Equation

Various solution algorithms and discretization schemes for the numerical solution of the NS-equation have been developed [22, 23, 88]. For example, as discussed in the theory part of the Publications, in Publications II-IV first order and in Publications V-VII second order accurate implicit time integration methods and are applied together with implicit treatment of convective and diffusive terms and semi-implicit treatment of the droplet momentum source term [22, 28, 29]. The spatial derivatives have been discretized with second order accurate numerical schemes. Furthermore, since the Mach number of the flow is mostly below 0.3, pressure needs to be treated in an implicit manner. The implicit discretizations lead to groups of algebraic equations. The symmetric algebraic groups of equations were solved using the Incomplete Cholesky Preconditioned Conjugate Gradient method whereas the non-symmetric groups of equations were solved with the Incomplete Cholesky Preconditioned Bi-Conjugate Gradient method. Although many algorithm variants exist, the basic idea of numerical solution of the incompressible NS-equation, in LES and DNS frameworks, is nowadays typically the so-called *fractional step* method that has been well described in the references [22, 88]. More information on the numerical algorithms of the present code are found in the literature [50, 83, 86].

3 Discussion of Results

3.1 Considerations on the Primary Atomization

General Aspects on the Dense Spray Regime: In the near-nozzle region the fuel spray is very dense and the liquid fuel to gas volume fraction $c = V_f/V_g$ is of order unity. According to the classical picture of the dense spray region, the liquid undergoes a primary atomization as follows: instabilities start to develop at the surface of the liquid core, the instabilities grow and finally the surface becomes very complicated in shape. At this point the liquid has transformed into large ligaments and droplets [1, 9, 10, 65, 66, 67]. In the downstream direction, as the liquid fuel to air volume fraction (c) decreases, the volume fraction of the voids correspondingly increases. At a certain point the intact liquid part must become fragmented but what is this point? The question has caused a lot of confusion in the diesel spray community but it is of great interest due to the important role of atomization to the fuel spray mixing. A novel argument on the nature of the intact liquid core length has been made by Roisman et al. [17] who state that in the fragmentation region the jet could be described as a cluster of randomly distributed liquid blops that occupy a relative volume c. Using results from the percolation theory, Roisman et al. argue that at a critical volume fraction $c^* = 0.311$ (in 3D) an infinite cluster of blops is broken and hence $c = c^*$ corresponds to the complete disintegration of the jet. It is clear that in a fuel spray c decreases below the values $c \sim 0.1$ within tens of injector diameters from the nozzle due to spreading of the spray.

X-Ray Measurements and RANS Spray Modeling: The background work for this thesis started in Publication I which is related to experimental near-nozzle diesel spray measurements using the x-ray technique. The experimental part was carried out at the Argonne National Laboratories and the fuel spray simulations

were carried out at the Helsinki University of Technology in the RANS-framework using the KIVA-code. The liquid core structure has been much investigated at the Argonne National Laboratories using an x-ray technique which reveals a 2D spatially and temporally resolved line-of-sight mass distribution as shown in Figure 3.1. It can be seen how the core of the jet breaks and starts to strongly spread within a distance of $2-3d_{inj}$. The radial line-of-mass integrated profiles are shown in Figure 3.2 which implies that values of $c \sim 0.3$ are noted at about $z = 50d_n$ downstream. It should be noted that here the gas densities is rather low ($1bar$ pressure and $293K$ temperature) and hence the breakup of the core is not extremely rapid. Further insight to the breakup of the liquid core can be seen in DNS of spray. For example, the direct numerical simulations by Lebas et al. [67] have implied that values $c < 0.311$ may be observed already at about $z = 20d_n$ downstream from the injector when the gas density is rather high ($\sim 30kg/m^3$).

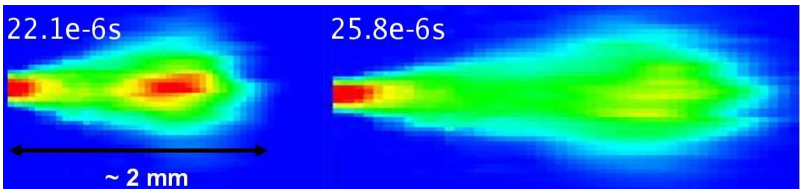

Figure 3.1: An x-ray line-of-sight mass density map of the near-nozzle region. In the experiment the gas density is low ($1bar$ pressure and $293K$ temperature). Courtesy of E.El-Hannouny and S.Gupta. Adopted from Publication I.

It is likely that the length of the 'continuos liquid core' (if present) depends on the gas density and injection pressure. In modern diesel engines the core does not exceed to distances longer than some millimeters (or tens of injector diameters) from the nozzle exit. In contrast, it is clear that the spray is very dense near the nozzle, and that, starting from the injector, there exists a complex transitional region from pure liquid fuel to a dense multiphase droplet laden gas jet in which four-way coupling effects have an important role. It is interesting to note that, as mentioned by Faeth, the breakup of the liquid core has many similarities with the

break-up of the potential core in the case of single phase jets [10]. In single phase jets the potential core is typically defined to be the downstream region within 4-5 inlet diameters from the inlet where the mean axial velocity remains constant. With laminar inflow conditions this means that the potential core is the most laminar part of a single phase jet. Outside the core the jet turbulence develops and eventually the shear layer merges at the end of the potential core and the flow becomes turbulent [48, 100].

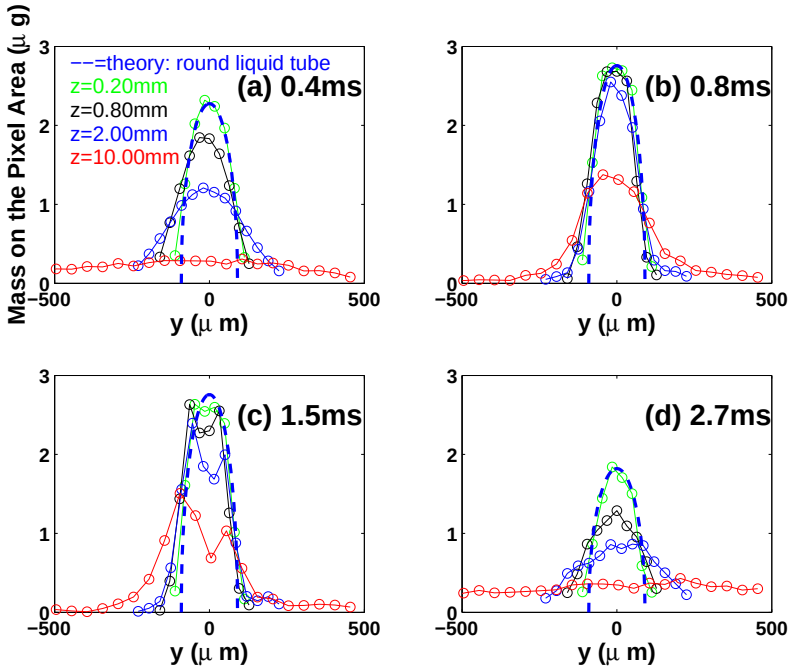

Figure 3.2: The line-of-sight mass at different downstream locations. The dashed line shows the theoretical mass distribution of a round liquid tube. Adopted from Publication I.

3.2 Droplet Size and Spray Shape

In a particle-laden multiphase flow, the particles and the carrier phase interact with one another. Faeth [10] names three aspects of droplet laden turbulent flows: 1)

drops are dispersed by turbulence, 2) the motion of drops modifies turbulence properties which is a reverse effect of turbulence on the drops, and 3) interphase transport rates (such as evaporation) are modified by effects of turbulence. Several authors have noted the dispersion effect: diesel spray shape can be significantly affected by the ambient conditions which affect also the droplet size [2]-[17]. Recently, there have been rigorous attempts to study particle dispersion using LES and DNS. Good examples are the studies by Luo et al. [40] and Yan et al. [42] where the authors used a plane jet as a base flow for such studies. The advantage is that such flows are rather easy to implement from the viewpoint of boundary conditions in contrast to e.g. the near-nozzle modeling difficulties. Hence, aside of experiments, LES and DNS together with LPT have become important tools in understanding the particle dispersion properties as they may reproduce the transient effects as seen in experiments.

Publications II-VII aim to bring insight to the PLJ problem since they all deal with explaining the effect of droplet size on spray cloud shape in particle laden jets at moderate mass-loadings $0.05 \leq \varphi \leq 1.3$. In Figure 3.3 a representative series of images, produced from the data of Publications VI-VII, is shown to demonstrate how droplet Stokes number St_p affects spray shape near the EOI in monodisperse sprays. The whole spray is depicted in the first column whereas only a cross-section is shown in the second column. It is noted that the spray images are qualitatively in line with the particle laden plane jet studies by Luo et al. [40] and Yan et al. [42]. The images also match the previous studies quantitatively from the viewpoint of St_p: large droplets with St_p of order unity have the most inertia and hence they tend to stay in the centerline until the potential core of the jet breaks and the flow becomes fully turbulent. After this the dispersion of the large droplets is also enhanced. In contrast, the small droplets have a small τ_p and they spread in a fog-like manner forming a mist that follows the fluid motions similar to the fluid particles.

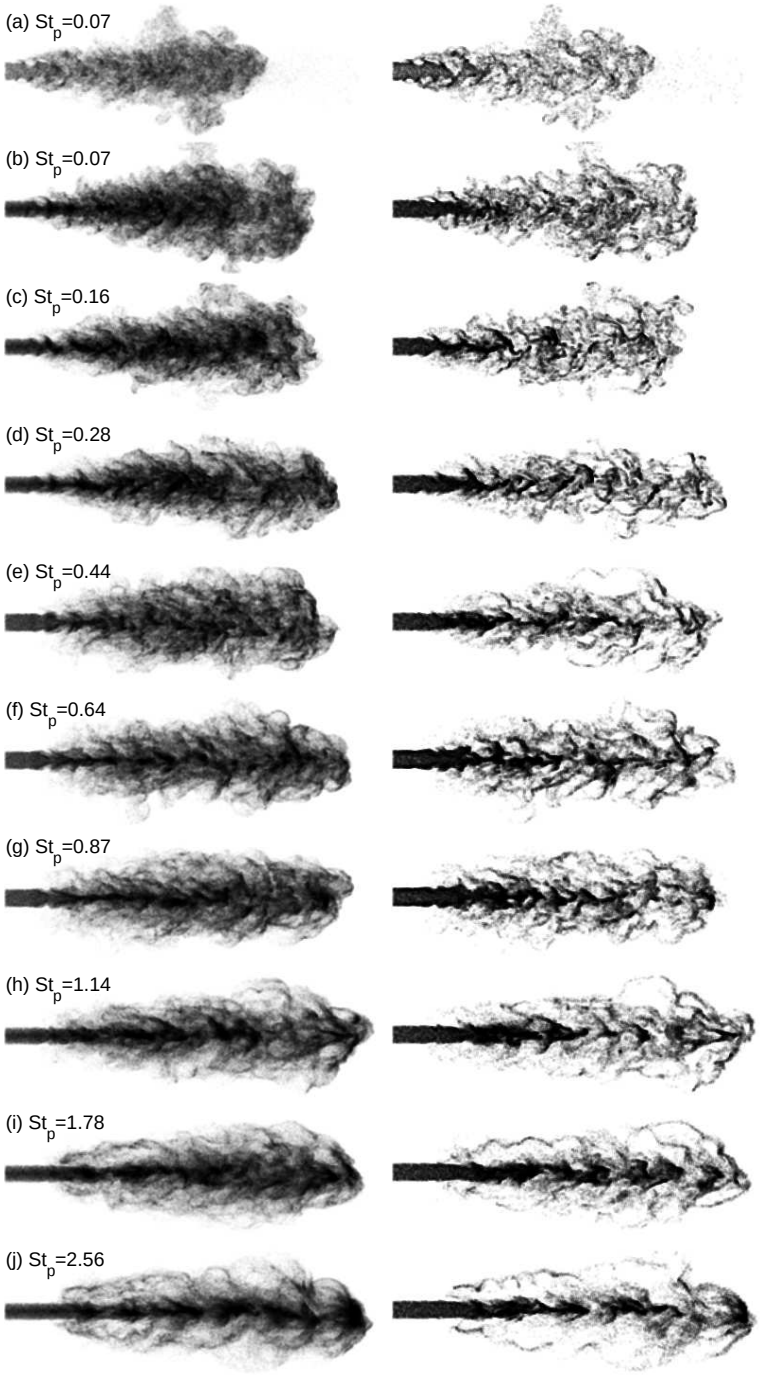

Figure 3.3: Large-Eddy Simulation of sprays. **(a)** Single phase jet with tracers. **(b)-(j)** Particle laden jets. **First column:** Whole spray near EOI is shown. **Second column:** Only a center-line cross section of the first column is shown. Adopted from the data of Publications VI and VII.

The picture is further clarified as the Figure 3.3 implies that the cross-over Stokes number between the two characteristic cloud shapes is approximately $St_p = 0.4 \pm 0.1$. Droplets may be considered to follow the turbulent motions considerably well if St_p is much below this range and they move rather independently if St_p is much above this range. In the cross-over range, especially when St_p is close to unity, the droplets are aligned in complex patterns (streaks) and, for example, it is possible to observe branch-like structures within the spray as seen in the second column of the Figure 3.3 at intermediate Stokes numbers. This kind of structures have been frequently reported in the context of diesel sprays (see [12, 18] and the citations therein).

The presented pictures match qualitatively the experiences from two-way coupling simulations within the mass-loading range $\varphi \leq 0.6$. However, the larger the mass-loading of particles becomes, the stronger the two-way coupling becomes. As was shown in Publications II-IV, increased mass-loading leads to prolongation of the potential core as the gaseous phase is being accelerated. This prolongs also the turbulence transition process further downstream. At lower mass-loadings ($\varphi \leq 0.3$) the potential core length is not prolonged very much. This is the situation seen in Figure 3.3 which forms an important starting point for further analysis of the spray data in Publications V-VII where a thorough quantitative and statistical analysis of the spray shapes is given

3.3 Connection Between Experiments and the Present LES

Spray shadowgraphy is a technique that can be used to take high-speed images of sprays together with back-light imaging [11, 12, 18]. The method captures the transient and irregular features of spray shape. Many authors have noted the similarities between sprays and jets and there exists a number of theories which aim to explain spray behavior in terms of gas jet theory [1, 2, 11, 25]. Here, the qualitative connection between particle laden jets and diesel sprays is demonstrated. Figure 3.4

shows side-by-side images of experimental non-evaporating diesel sprays (right) and simulated particle laden jets (left). In Figure 3.4 the dense spray part is not simulated but taken from the experimental picture to better understand the connection. Although different in many ways, the correspondence between the simulated sprays and experimentally observed sprays is apparent. For example, LES reproduces the transient and random nature of fuel sprays as seen in the experiments. Also the spray angle is similar to the experimental angle when the droplets are small because of 'natural' dispersion by turbulence which spreads the jet. This effect is important since the spray opening angle is not modeled.

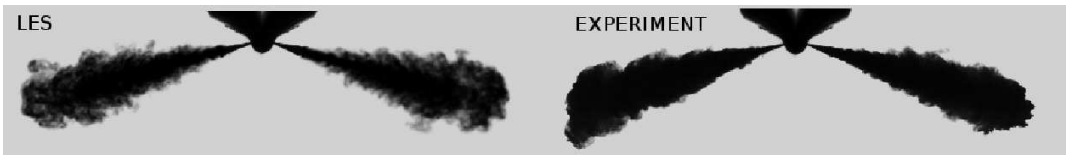

Figure 3.4: Qualitative comparison on the spray shapes as obtained with LES (left) and shadowgraphy (right). In the LES the initial part of the spray is not simulated. Adopted from the data of Publications V-VII.

In addition to shadowgraphy, we have also used the laser-sheet imaging technique to gain insight to the internal structure of the fuel spray (see [18] for further details). Figure 3.5 gives a qualitative comparison of the structure of experimental spray vs current LES and demonstrates that, although different in many ways, the same physical phenomena are present. For example, it is possible to observe that the spray structure is heterogenous. Droplets are more concentrated in certain parts of the flow and the phenomenon is closely related to the eddies in the shear layer and the interaction of droplets with the eddies. Also voids inside the spray can be seen as well as large droplets that are clearly observed in the outer periphery of the spray. Thus, Figure 3.5 reveals that LES reproduces certain aspects of droplet-eddy interactions as seen in the experiment and thus LES has the potential to mimic the transient nature of spray-turbulence interactions.

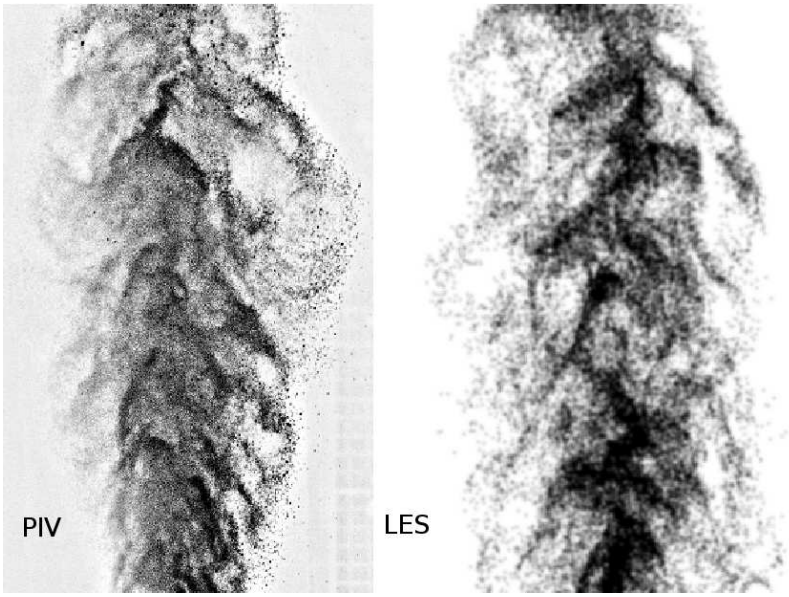

Figure 3.5: Qualitative comparison on the random structure of polydisperse sprays with PIV (left) and LES (right). The LES data is adopted from the data of Publications VI and VII.

3.4 Effect of Atomization

In Publications I and V the secondary atomization of droplets is considered. Secondary breakup is typically referred to when droplets atomize due to aerodynamic interactions. However, in Publication V also oscillatory resonance breakup is considered in turbulent conditions at low Weber numbers. Two non-dimensional numbers that are of importance to secondary atomization in non-evaporating sprays are the Weber number (We) and the Ohnesorge number (Oh). The Weber number is defined as the ratio of aerodynamic drag and surface tension forces whereas the Ohnesorge number is defined as the ratio of aerodynamic drag to viscous forces (see e.g. [9, 10]). Faeth [10] has presented a phase diagram covering a wide range of data demonstrating how, for a given Oh, different secondary breakup regimes may be noted. At low Oh, as typical in fuel spray applications, at the critical Weber number of $We_c \approx 12$, droplets become unstable and may break via the *bag breakup*

mechanism where the droplets stretch into a bag-like structure and then break. As We increases, very complex breakup regimes can be observed [9, 10]. Further aspects of secondary breakup, such as temporal properties during the breakup cascade at different breakup regimes, considerations on the child droplet size/velocity distributions immediately after the breakup or considerations on the timescales of droplet breakup, are given by various authors, e.g. [58]-[60], [64].

It has been noted that in diesel spray modeling an important aspect is to delay the droplet breakup process until droplets have propagated long enough i.e. reached a breakup-length [24, 25]. This effect was demonstrated also in Publication I using two standard breakup models. The experiences of this preliminary study, together with literature, implied that LES is needed to understand the dynamic nature of droplet-gas coupling as the method captures the transient nature of flow fields. Publication I also showed that the breakup models have non-linear details which might complicate the outcome of a simulation. Thus, the decision was made to not to model the droplet breakup in the Publications II-IV, VI and VII.

To some extent, the issue of droplet breakup modeling is further discussed in Publication V in which it is noted that most of the currently existing LPT spray submodels have been originally tailored and calibrated on the purpose to be applied within the RANS-framework. Hence, it is natural to expect that the conclusions that are drawn from the functioning of any spray sub-model depend also on the turbulence modeling approach. Thus, in Publication V a simple atomization model is presented that can be used to control the spray shape and breakup length especially in the low-Weber number regime.[1]

Figure 3.6 shows the effect of atomization to the breakup length. In the upper panel the situation is similar to a case when the spray is immediately atomized into very

[1]In typical CFD-simulations, if rapid primary breakup into small droplets is assumed, one is easily left with huge parts of the spray that are in the low We regime.

small droplets which is modeled by injecting monodisperse droplets ($d = 2\mu m$) without the breakup model. In the lower panel the initially large droplets ($d = 12\mu m$) break slowly which can be seen as a prolongation of the breakup length. Hence, the dispersion starts to form later as the Stokes numbers of the droplets gradually decrease. For a qualitative comparison, Figure 3.7 shows how an experimental fuel spray develops in time.

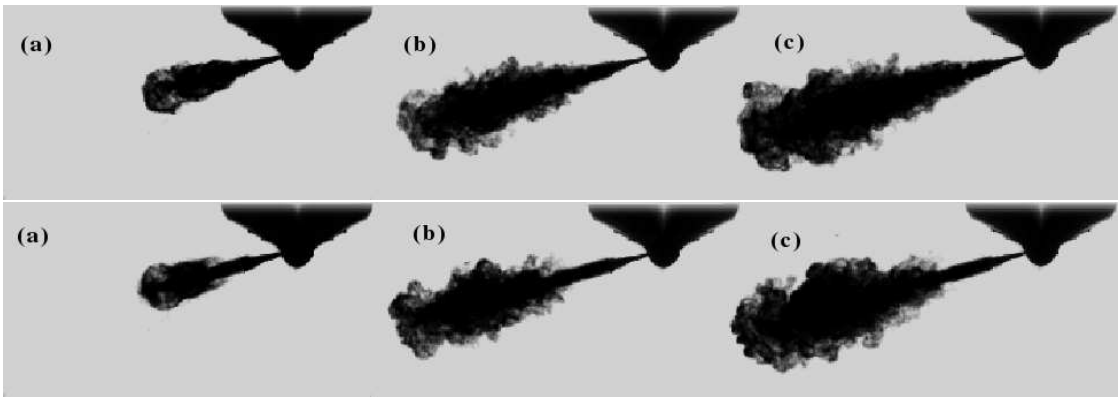

Figure 3.6: Large-Eddy Simulation and comparison of time development of sprays in two simulated cases. **First row:** Small monodisperse droplets that are dispersed well. **Second row:** Large droplets that undergo breakup leading to enhanced dispersion later downstream. The length of the spray at the latest time is approximately $40mm$. Adopted from Publication V.

Figure 3.7: Typical experimental spray patterns as observed in non-evaporative, high pressure diesel spray experiment. The length of the spray at the latest time is approximately $40mm$. Adopted from Publication V.

The atomization model of Publication V corresponds to assuming that a parcel size evolves in a stochastic way according to the Poisson process [89]. Importantly, this

assumption is in contrast to other existing breakup models where droplets inside a parcel are assumed to oscillate/deform/break in a deterministic manner in the same phase. The number of parcels at time t in a certain size group evolves dynamically in time according to the following set of ordinary differential equations:

$$\begin{cases} \frac{dn_0}{dt} = -\lambda_0 n_0(t) + \mathcal{S} \\ \frac{dn_k}{dt} = +\lambda_{k-1} n_{k-1}(t) - \lambda_k n_k(t) \\ \frac{dn_N}{dt} = +\lambda_{N-1} n_{N-1}(t), \end{cases} \tag{3.1}$$

where each droplet size is associated with the size class index $k = 1, ..., N-1$ and λ_k is the breakup rate for droplets of size class k. Each breakup event splits a droplet volumwise in half and thereby reduces drop diameter by factor 0.80 assuming identical child drop radii. The source $\mathcal{S}$ corresponds to the rate at which parcels enter the chamber ($\mathcal{S}$ having units parcels per time step). The model produces a discrete spectrum of droplets and λ_k depends on droplet size. In Publication V, λ_k is associated with droplet oscillation frequency which may trigger droplet breakup at low Weber numbers via resonance [9]. Finally, it is noted that the Eqs. (3.1) admit a stationary state solution by setting $\frac{dn_k}{dt} = 0$, for $k < N$.[2] The stationary parcel number distribution can be observed after rather long times have elapsed.

3.5 Spray Penetration

Spray tip penetration, as a function of time, is perhaps the most common quantity to study in the field of diesel spray research since the tip position can be easily detected from spray shadowgraph images [1, 11, 17, 18, 24]. To understand how the spray cloud develops on average we define the spray penetration as the following RMS value $S(t) = \sqrt{\langle z_p(t)^2 \rangle}$. Here the brackets $\langle . \rangle$ denote averaging over all the droplets in the cloud at a given time and z_p is the parcel's instantaneous $z-$coordinate. It should be pointed out that the given definition for $S(t)$ is an average penetration

[2] $\frac{dn_N}{dt} > 0$ as the amount of the smallest droplets is defined to be increasing (they are assumed stable).

that can not be detected from shadowgraph images. Yet, $S(t)$ may be considered to be a measure of the spray cloud behavior as whole in contrast to the tip penetration.

Figure 3.8 shows that the droplets with increasing St_p have a stronger penetration but the St_p dependency is still rather weak: when St_p increases by nearly two orders of magnitude the penetration changes only by some tens of percents. The right panel shows the data plotted as a function of a dimensionless variable $\xi = (t/T)^{\eta_t}(d/D)^{\eta_d}$. By trial and error, it is noted that the data collapses on a single curve which is nearly a linear function and it is approximated that the exponent $\eta_t \approx 0.65 \pm 0.05$ and the exponent $\eta_d \approx 0.15 \pm 0.03$. It is interesting to note that in comparison to other theories on e.g. diesel spray tip penetration (see [1]) a slightly larger exponent $\eta_t > 0.5$ is observed here. This seems natural since the value $\eta_t = 0.5$ corresponds to fully random motion i.e. similar to a cloud of particles undergoing Brownian motion (diffusion). Here, in contrast, a strong axial momentum stream is present and it is natural to expect that $\eta_t > 0.5$.

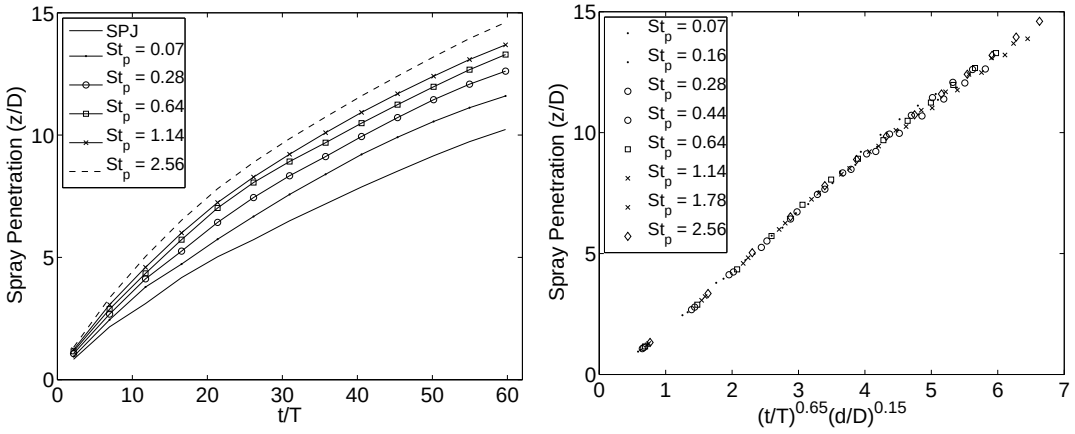

Figure 3.8: Spray penetration defined as the RMS of droplet cloud z-coordinate. Droplets with increasing St_p have a stronger penetration. The lower panel suggests that the penetration is a function of the form $S = S(t^{0.65}d^{0.15})$. Adopted from the data of Publications VI and VII.

3.6 Flow Structures

Many experimental studies of fuel spray injection have shown that vortex-ring like structures can be observed in the spray tip region [12]-[14], [17]. Some authors have related the appearence of soot emissions inside diesel sprays with the tip vortex [2]. There is also experimental evidence that the Sauter mean diameter (SMD) of the droplets at the outmost periphery of the spray might be larger than that of the droplets near the spray axis [7, 98]. It has been suggested that this phenomenon would be related to the interaction of the large droplets with the tip vortex which would centrifuge the droplets away from the spray axis [98]. Hence, an interesting question to be answered is related to the appearance of the vortex structures within the spray regime together with the interaction of droplets with these structures.

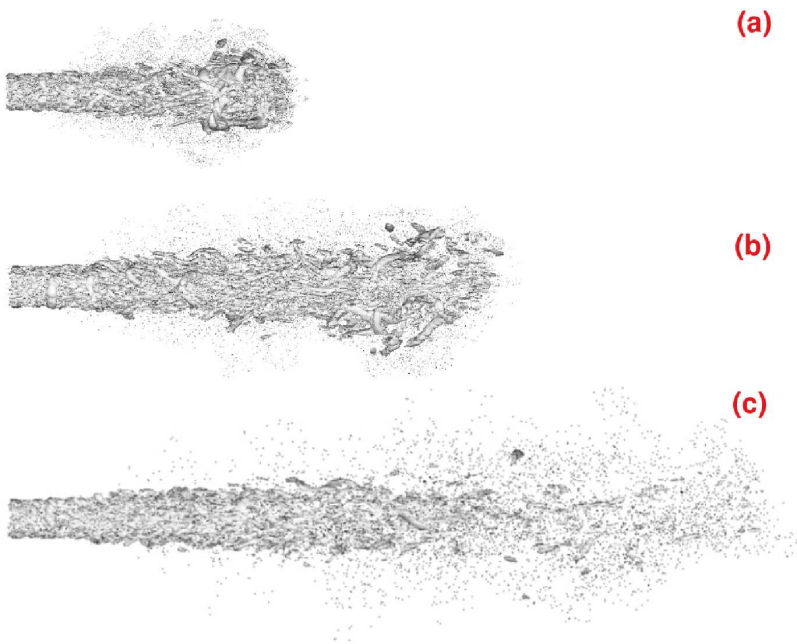

Figure 3.9: Snapshots of time evolution of vortical structures visualized by the Λ_2 criterion [101] together with small droplets. The small droplets are noted to form a fog-like cloud. Here $\varphi = 1.3$ and $d = 2\mu m$. Adopted from Publication II.

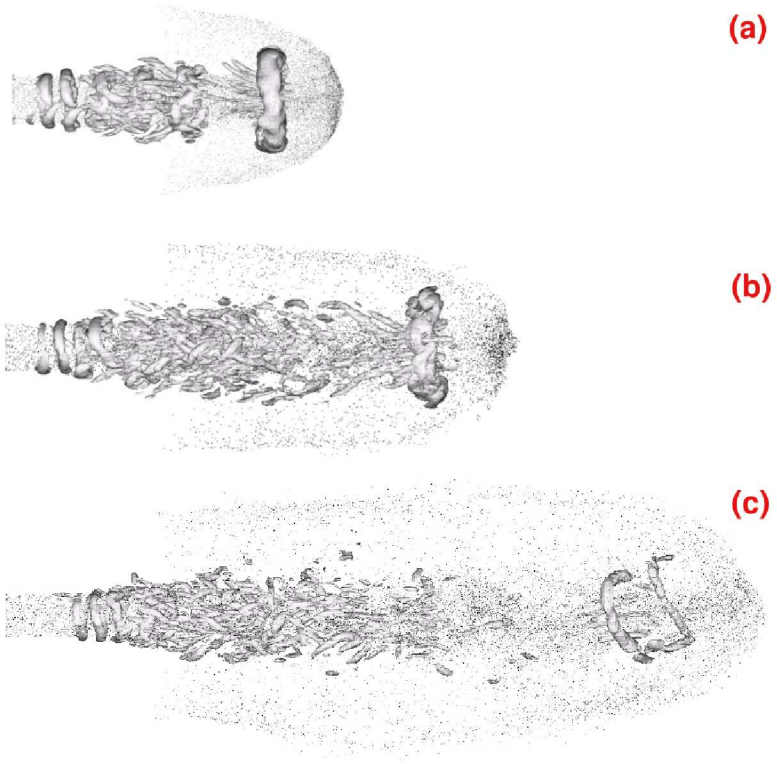

Figure 3.10: Snapshots of time evolution of vortical structures visualized by the Λ_2 criterion [101]. The large droplets are noted to first form a mushroom-shaped cloud which breaks at later times. Here $\varphi = 0.1$ and $d = 20\mu m$. Adopted from Publication II.

In Publication II one of the background motivations is to seek such injection conditions from the computational model where 1) the tip vortex is observed, and 2)) the tip vortex is not observed. Also, it was of interest to seek for conditions where 1) the turbulence is highly dissipated, and 2) the turbulence dissipation is not very strongly affected. One option to see these contrasting situations in the computational model is to vary the mass-loading (φ) and droplet size (d). Hence, the effect of high mass-loading ($\varphi = 1.3$) of small particles is tested against a low mass-loading ($\varphi \leq 0.10$) of large particles. Figures 3.9 and 3.10 show two different droplet clouds together with the isocontours of Λ_2 (see text below) [101]. It can be seen that at small mass-loading of large particles a clear doughnut shaped tip vortex forms. The vortex is characteristic to single phase jets and the droplet interactions complicate

the dynamics of this vortex [48, 49]. For example, it is seen that the vortex becomes unstable, it then deforms and eventually breaks after $z/D = 10$ downstream which leads to enhanced dispersion of droplets. This phenomenon is similar to that reported by Sankaran et al. [34] who noted that, in a combustor simulation, increase in jet swirl number drastically increased droplet dispersion later downstream as coherent large scale flow structures were subject to complicated stretch effects and consequent breakdown. Other examples of break-down of vortex structures using implicit LES have been previously presented in the literature [19, 20, 49]. However, the important observation is that the interaction of the droplets with the tip vortex leads to a spray cloud that has a mushroom shape. The vortex visualization using the Λ_2-criterion has been quite popular and it is related to the computation of the second largest eigenvalue of the symmetric tensor $\mathbf{S}^2 + \mathbf{\Omega}^2$. where $\mathbf{S}$ and $\mathbf{\Omega}$ are respectively the symmetric and the antisymmetric parts of the velocity gradient tensor. Λ_2 has been noted to accurately identify the vortex cores in flows where the vortex geometry is intuitively clear [101].

The small droplets, having small Stokes numbers, form a cloud that is of different character than the cloud with large droplets. In contrast to large droplets, a high mass-loading of small particles inhibits the formation of the tip vortex as seen in Figure 3.9. This phenomenon reflects the general findings of this work also regarding the later Publications III-VII: even reasonable mass loadings ($0.15 \leq \varphi$) of small droplets may inhibit the formation of the tip vortex. However, the most apparent consequence of high mass-loading of particles which have a higher velocity than the incoming gas is to increase the length of the potential core due to axial momentum source. In addition to that, as the Publication II shows, another consequence of adding small particles is that turbulence levels may stay at a low level in the near field of the jet and the full transition into turbulence is prolonged further downstream. This is in contrast to single phase jets and particle laden jets with low mass-loadings for which the potential core breaks around $z/D = 4$. In this way, the examples of Publication II imply that small droplets may be harmful to the mixing process if

there are too much of them in a fuel spray.

To summarize, this study implies that in droplet laden jets the tip-vortex can be observed in accordance with single phase jets. The tip vortex is formed at early times due to the strong entrainment of the jet into the quiescent gas. However, the findings imply that St_p and φ have an important role to the formation of the vortex. Especially, when $St_p \ll 1$ the tip vortex was not clearly observed (or, it decayed rapidly) if $\varphi \sim 0.1 - 1$ due to two-way coupling: strong interactions near the near inlet inhibit the formation of the vortex. If $\varphi \ll 0.1$ the tip vortex is clearly observed since the two-way coupling effects are weak. If $St_p \sim 1 - 10$ and $\varphi \sim 0.1$ the tip vortex was typically observed much more clearly than at lower Stokes numbers.

3.7 Visualization of the Kelvin-Helmholtz Instability

Flow Character: Several studies where time-averaged statistics of the near-field and the far-field (i.e. self-similar) regions of jets and particle laden flows can be found in the literature [8, 39, 45, 46, 90, 91, 93, 101]. Studies which have mostly concentrated on transient analysis of particle laden flows can also be found from the literature [40]-[42]. In this work a transient flow with a momentum source is considered and the analysis is based on time dependent data. This is also an inherent part of the real world sprays since in fuel spray applications the spray tip propagates constantly and hence, by definition, diesel sprays are inherently transient and the average values depend on time. Nevertheless, as explained in the text below, there are certain commonly known features regarding jets that can be visualized and analyzed by means of Fourier analysis in the present problem.

Shear Layer Instability: Starting from the inlet, vorticity is produced in the shear layer of the jet which results in the merging of the shear layer at the end of the potential core around $z/D = 4$ [48, 49, 90, 91]. The potential core length is

considered in Publications II-IV. The shear layer growth and the related turbulence transition process is visualized in Figure 3.11 by injecting a passive scalar c from a narrow region at the inlet along the shear layer. Physically, the passive scalar corresponds to marking the fluid with a small amount of e.g. dye or smoke which is assumed not to interact with the flow itself. Under these assumptions, the passive scalar evolves according to Eq. (2.6) which is solved in the flow domain using a flux limiter for the convection term. The limiter ensures the scalar to be bounded between physically and mathematically feasible values ($0 \leq c \leq 1$).[3] The boundary condition for the passive scalar is given by setting $c = 1$ along the annular region at the inlet. This visualization method was used earlier by Ding [92] and it is a visually attractive alternative in contrast to injecting the passive scalar uniformly from the whole inlet area since the development of the shear layer can be well seen.

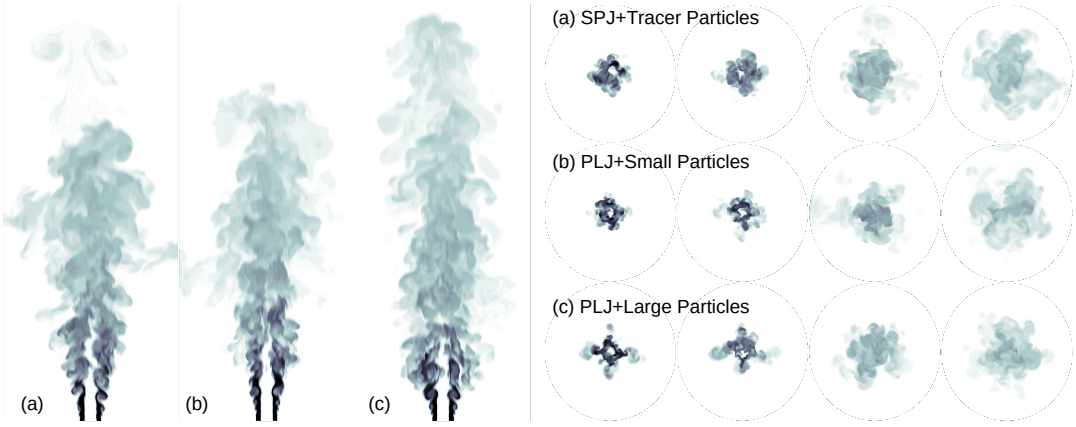

Figure 3.11: Passive scalar visualization by injecting the scalar from an annular region along the shear layer of the jet. Droplets are not visualized. **Left:** The growth of Kelvin-Helmholtz instability and merging of the shear layer is visualized. **Right:** The jets are coming towards the observer. Visualization from four different downstream positions. Adopted from the data of Publications VI and VII.

The passive scalar also clearly visualizes the growth of the classical Kelvin-Helmholtz-instability which is caused by the destabilizing effect of shear, which overcomes the stabilizing effect of stratification and the instability forms in between the two fluid

[3]It can be proved mathematically that the passive scalar is bounded in the domain [8].

layers that move with different velocity (here: the jet and the quiescent air) [99]. In the case of homogeneous fluid (a vortex sheet) linear stability analysis can be used to show that the vortex sheet is always unstable to all wavelengths. Further discussion on the KH-instability and visualization similar to Figure 3.11 can be found in the reference [99]. However, in diesel sprays, the Kelvin-Helmholtz instability is of importance due to the developing shear layer of the spray. For example, Edwards et al. [98] have employed high speed visualization to study autoignition of a transient spray under diesel-like conditions and the ignition was observed to be initiated in large vortex structures that are generated due to the KH-instability [97].

Velocity Spectra: In order to simulate a turbulent flow a range of spatial and temporal scales need to be resolved. For example, for a turbulent jet, it is immediately clear that the grid resolution needs to be at least $D/10$ to resolve the kinetic energy of the small turbulent eddies i.e. to have a scale separation between the large and the small scales. In fact, Olsson and Fuchs have estimated the Taylor microscale [8] for jets at $Re = 10^4$ to be of order $\sim D/5$ [48]. Furthermore, as the spatial resolution is refined and the large eddies are thereby allowed to break into smaller eddies, energy is transferred from slowly evolving frequencies to the high frequency components of the solution. Numerical stability may be achieved if energy is not accumulated to the highest frequencies i.e. energy is dissipated at the small scales quickly enough. In ILES this can be achieved by dissipative numerical discretization. However, the numerics should not 'contaminate' the large scale eddies by being e.g. overly dissipative and hence not all ILES will work [8, 46]. In the present study it was noted that the afore-mentioned criteria are satisfied if the convection term is discretized properly with a second order accurate centered scheme and if the second and first order implicit time integration methods are used. In contrast, *contamination of the large scales* by numerics may be observed if the convection term is discretized inadequately since, for example, the potential core of the jet may apparently break too fast in contrast to what is known from the literature. However, as Publication IV briefly shows, the used discretization method predicts the potential core length

adequately together with approximate decay rate which is in line with the literature (c.f. [48] and the citations therein).

The velocity spectra are considered in Publication II where it is shown that the spectra might be affected by the presence of particles/droplets. Here, a re-check on the spectra is made using the data of Publications VI and VII as the simulations are more comparable with one another. Figure 3.12 shows that the spectra of radial velocity component along the shear layer of the jet are rather similar for the SPJ and PLJ when the droplets are large. In specific, in the near field at $z/D = 1.5$ the characteristic frequencies of the jet can be seen as peaks in the spectra [48, 49]. These peaks can be related to the shear layer instability which is of Kelvin-Helmholtz (KH) type as visualized in Figure 3.11. Further downstream at $z/D = 4.5$ the vortex merging process has nearly by-passed via ending of the potential core and hence the spectra look smoother. However, it is noted that the spectra may be affected by the presence of small droplets: at $z/D = 1.5$ the characteristic frequencies are not seen as clearly as in the other cases when droplets are larger which is an implication of strong interaction of small droplets and small eddies.

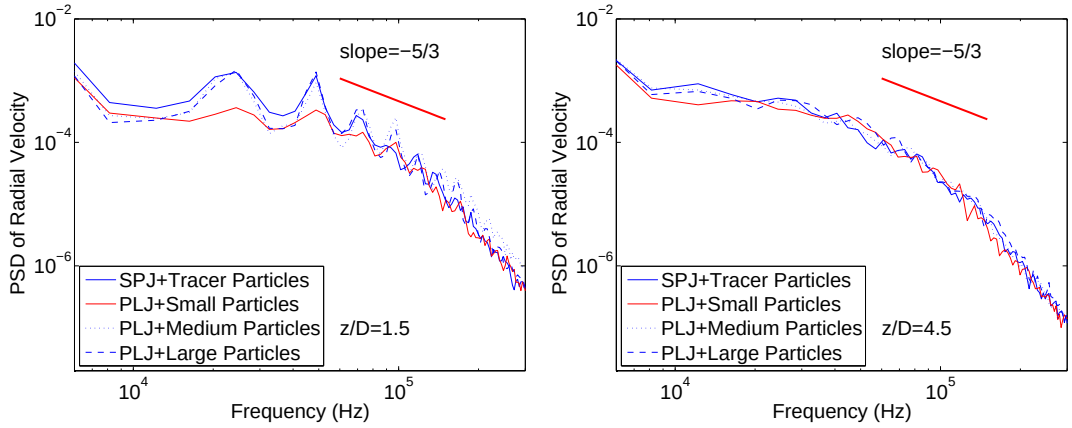

Figure 3.12: Spectra of radial component of velocity at two downstream locations along the annular shear layer. The spectra were constructed using the *Welch's* periodogram method based on the FFT-algorithm. **Left:** $z/D = 1.5$. **Right:** $z/D = 4.5$. Adopted from the data of Publications VI-VII.

3.8 Droplet Level Information and a Statistical View on Sprays

A statistical understanding on the visual observations on spray shapes is needed to better understand the two-way coupling. Starting from Publication IV, it is deduced that: *the spray cloud shape must be explainable using the statistics of the spray momentum source term.* Namely, as the droplet equation of motion depends on the slip velocity according to Eq. (2.11), it is shown in Publication IV that the PDF of the radial and axial components of $\mathbf{u}_g - \mathbf{u}_p$, much depend on the droplet diameter and the Stokes number. The corresponding PDFs, as seen in Figure 3.13, are also considered in Publications V and VI. Furthermore, the distribution of the radial component of $\mathbf{u}_p$ explains the differences in spreading and, hence, the differences in spray cloud shapes. As the findings of Publication IV were done with a first order time integration scheme, a full assesment of the related PDFs together with a careful Stokes number study is done in Publications VI using a second order accurate time integration scheme.

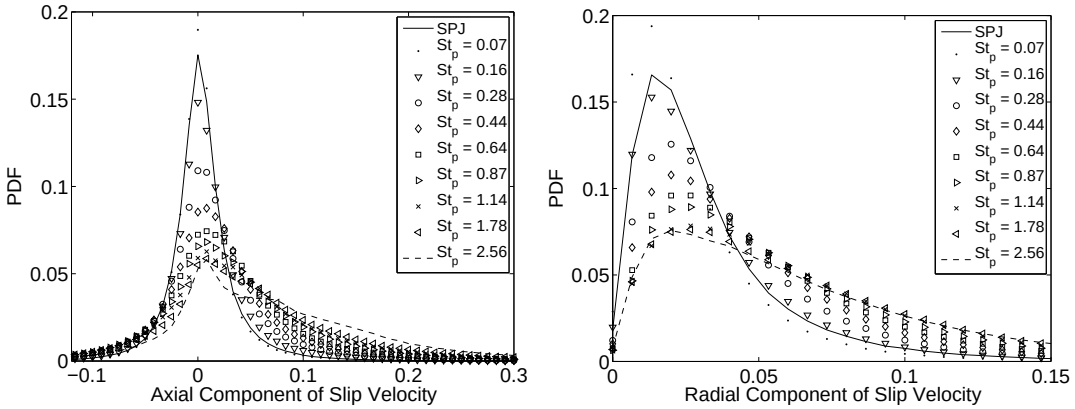

Figure 3.13: **Left:** PDF of axial component of slip velocity near EOI. **Right:** PDF of radial component of slip velocity near EOI. Note that PDFs for the droplets with higher St_p are more shifted to the right than the PDFs for the small droplets. Adopted from the data of Publications VI-VII.

At SOI, the PDF of droplets' velocity is ideally a delta-function because all the

droplets are injected with the same initial velocity. The slip velocity distribution at SOI is a narrow uniformly distributed peak which only depends on the inlet random velocity fluctuation. During injection the PDF evolves in time: new droplets are introduced to the system at a constant rate whereas droplets adapt to local flow conditions on the timescale τ_p. A droplet interacts with an eddy if the eddy turnover time is close to τ_p. The time evolution of the droplet-level PDFs should have a strong role on spray cloud formation since the droplet velocity and especially slip velocity statistics determine the strength of interphase coupling.

3.9 Mixing

3.9.1 Preferential Concentration vs Mixing

A commonly reported phenomenon in particle laden flows is the so called 'preferential concentration' [71, 74, 78]. The phenomenon refers to the tendency of particles of certain size to accumulate in certain regions of the flow. Hence, particles that are initially distributed homogeneously may gather closer together into correlated clusters. It has been reported that the strength of the phenomenon correlates with St_p [34, 54, 71, 72, 74, 77, 78]. It has been noted that the favorable regions might be those where the vorticity is low and the rate of strain is high [71].

In sprays two characteristic factors that influence the mixing process are 1) spreading, and 2) turbulence originated mixing. Hence, the average interdroplet distance becomes larger when going downstream and the spray becomes more dilute. Thus, the nature of preferential concentration in sprays is different to that in homogeneous turbulence. In Publications III-VII the mixing and internal structure of sprays is studied. Figure 3.14 demonstrates that the internal structure of an experimentally observed spray may contain voids and heterogeneous droplet distribution. Impor-

tantly, due to spreading, this structure is not formed due to droplets literally 'clustering' together but more likely due to the fact that the initially dense parts of the sprays are not properly mixed. Thus it is likely that the droplets inside the heterogeneous, streak-like regions were close to each other already near the injector. Figure 3.14 shows the structure of two monodisperse LES/LPT sprays. It is seen that the mixing is very different between the medium sized and small droplets. It is seen that, when the Stokes number is rather large (of order unity), regions that are empty of droplets (voids) appear. In fact, the larger droplets tend to follow the large scale (low frequency) motions of the fluid as is explicitely shown in Publication V by analysing the droplet-wise velocity and slip-velocity spectra. The effect is also partly seen in Publications IV and VI by analyzing the slip velocity statistics. In contrast, the small droplets form a mixture that fills the spray volume rather uniformly. It is important to understand that such great changes in the mixing pattern depend strongly on St_p.

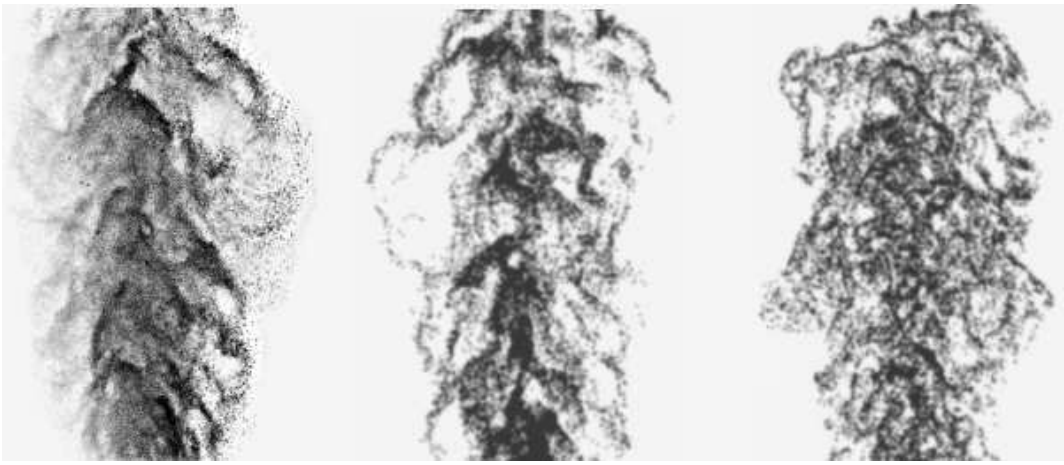

Figure 3.14: Qualitative comparison on the random internal structure of sprays and the preferential concentration of droplets. **Left:** Experimental PIV measurement. **Middle:** LES, medium size droplets with $St_p \sim 1$. **Right:** LES, small droplets with $St_p \sim 0.1$. The depicted spray regions are about 10mm by 25mm in size near EOI from the tip region of the sprays. Adopted from the data of Publication VII.

3.9.2 The Basic Definition of Mixing

Conventionally, the mixing problem is studied by e.g. measuring the average or rms value of passive scalar consentration in a flow field. In the spray problem it is possible to also consider other means because the coordinate data of the Lagrangian point particles is directly available in contrast to experiments offering thereby flexibility and new ways of considering the mixing problem. To understand the mixing process better we seek for a clarifying statistics which would indicate mixing quality. Consider N spheres that are labeled by an index between $1...N$ and drop them into a box so that sphere number 1 enters first, sphere number 2 enters second and so on. If the box is not shaken the spatial configuration of the spheres inside the box (after the sphere N has entered) is correlated with the initial configuration of the spheres. Hence, it is more probable to find e.g. the sphere number n in the vicinity of sphere number $n + 1$ than in the vicinity of sphere number $n + 10$. However, if the box is shaken *mixing* takes place and after a long enough time the spheres are randomly distributed. A quantity that indicates the level of mixing is the *local standard deviation of sphere number* inside a small sub-volume in the box: the larger the standard deviation, the better the mixing.

3.9.3 Mixing Indicator Using Droplet Residence Time Concept

The previous example applies to sprays as well and it is possible in LES, in contrast to experiments, to actually use this basic definition of mixing as follows: if each droplet is labeled according to the time the droplet started from the inlet, i.e. t_{start}, it is possible to compute (for each droplet separately) droplet residence time τ_{DRT} in the chamber at time t simply as:

$$\tau_{DRT} = t - t_{start},\ t \geq t_{start}. \tag{3.2}$$

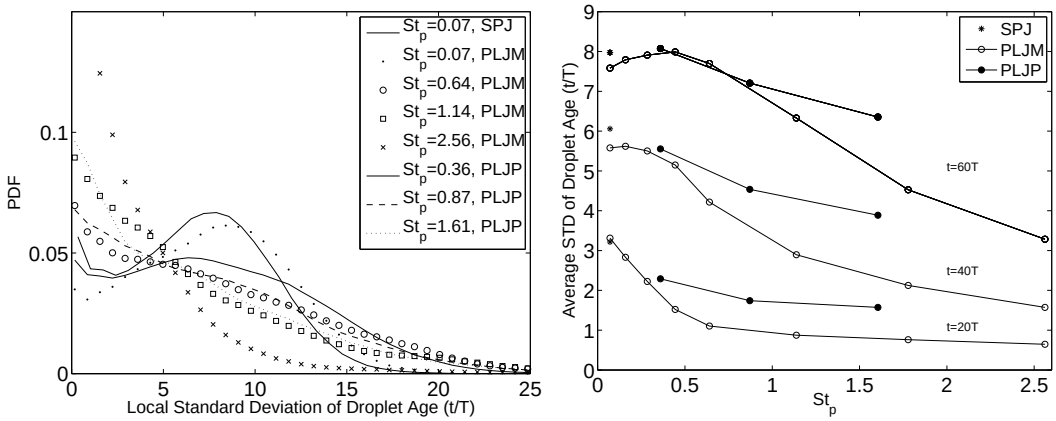

Figure 3.15: **Left:** PDF of local standard deviation of droplet residence time. **Right:** Average standard deviation of DRT. Adopted from the data of Publications VI-VII.

Thus, it is possible as a post-processing task to compute the field of standard deviation of the variable τ_{DRT}, i.e. $\sigma_{DRT} = \sigma_{DRT}(x, y, z, t)$, on a properly chosen length scale. This can be done by dividing the flow field into rather small (but not too small) subvolumes (cubes) and then compute σ_{DRT} in each of the cubes. The approach is straightforward and it has been explained thoroughly in Publication VII. From Figure 3.15 it is seen that the large droplets are not dispersed very much and thereof their initial configuration changes slowly. Thus, the corresponding PDF is highly concentrated to low values and also the average $\langle\sigma_{DRT}\rangle$ is low indicating that two droplets are not likely to come near each other if they were injected a long time apart i.e. mixing is inefficient. In contrast the same PDF for the small droplets is much more symmetric and upward-shifted and hence the small droplets can be deduced to mix well. The right panel of the Figure 3.15 shows the dependence of $\langle\sigma_{DRT}\rangle$ on time and St_p. It is seen how the mixing is improved as time proceeds and that the small droplets mix much better than the large ones. At EOI the monodisperse small droplets have mixed by factor 2.6 better than the large droplets. The experiences of this study imply that $\langle\sigma_{DRT}\rangle$ explains consistently mixing differences in monodisperse and polydisperse sprays.

3.9.4 Mixing Indicator Using Droplet Group Expansion

Formally, in an isotropic environment (say: homogeneous and isotropic turbulence), diffusivity of a particle group can be defined by squaring the 'width' of the group and dividing this number by the elapsed diffusion time [8]. In Publications V-VII the formal procedure is applied in the spray context in order to quantify the differences in spray shape and mixing. This is done by associating a diffusion coefficient $\Gamma = \Gamma(St_p)$ with the studied sprays. One way to do this, the total injection time being $60D/U_o$, is to first divide the sprays into 60 droplet groups according to the time window the droplets started from the inlet and study how the width of the droplet groups increases when droplets mix. The mixing of one droplet group at three different times is visualized in Figure 3.16.

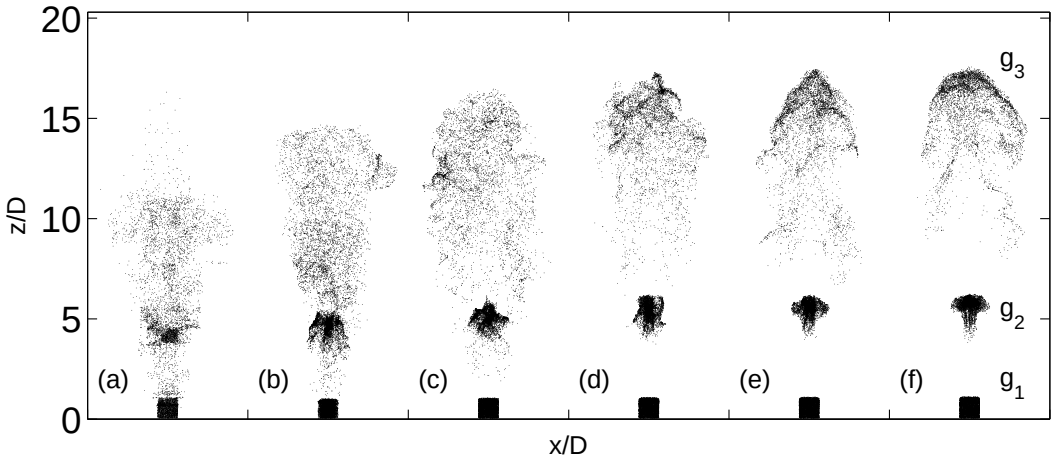

Figure 3.16: Time-evolution of a monodisperse droplet group that started around time $t = 10T$ is shown. The same (≈ 6000) droplets at three different instances of time are shown. The full spray consists of 60 groups but here only one of the groups is visualized. The volume of the group grows in time so that g_1 corresponds to the group close to time $t = 10T$ and the smallest volume and g_3 corresponds to the group close to the latest time with largest volume. **(a)** SPJ ($St_p = 0.07$), **(b)** PLJ ($St_p = 0.07$), **(c)** PLJ ($St_p = 0.28$), **(d)** PLJ ($St_p = 0.64$), **(e)** PLJ ($St_p = 1.14$) and **(f)** PLJ ($St_p = 2.56$). Adopted from the data of Publications VI-VII.

The visualization implies that large droplets do not mix efficiently until the spreading begins rather late downstream. As explained in Publication VII, the final volume of the group at EOI, i.e. V, can be defined for each group separately using the streamwise and cross-streamwise group dimensions (i.e. length and width). This leads to definition of an average length scale $L = \langle V^{1/3} \rangle$ by averaging over all droplet groups. A turbulent diffusion coefficient for the whole spray may then be evaluated by squaring the length scale and dividing this number with the elapsed time i.e.

$$\Gamma = L^2/\tau_{inj}. \tag{3.3}$$

Note that here the same timescale τ_{inj} is used for each droplet group to represent an average time although Γ could be defined in many other ways as well. Instead of Γ, one could equally well use V as an effective measure of volumetric interactions but here Γ was chosen in order to connect the mixing index with turbulent diffusion.

The results of Publications V and VII indicate that at EOI the smallest monodisperse droplets may have 60% higher Γ than the large droplets and hence the small droplets can be well mixed by the turbulence. In spray combustion it is desirable that the air inside the spray is fully utilized. A 60% increase in Γ translates to 100% change in droplet group volume which implies that there is clear potential in utilizing the air inside the spray more effectively if the droplets are small in comparison to the droplets being large. In other words: 50% of the air may remain unused inside the fuel spray if droplets are too large in comparison to being small. This observation clearly seen from the spray structure visualization in Publications V-VII. The observation is also much in line with the experimental observations which imply that smaller nozzle diameter and higher pressures may yield smaller droplets [1, 6, 7, 11]. In summary, spray shape is related to mixing the strength of which can be quantified in terms of Γ. Turbulence disperses the smallest droplets the best because: (*i*) They have a small St_p. (*ii*) The mass-loading of the small droplets is rather small and hence turbulence dissipation is low. (*iii*) The jet base flow does not exhibit very strong shear layers which could affect the mixing.

4 Summary

4.1 Summary of the Publications

Publication I is related to analysis of near-nozzle x-ray data and RANS turbulence modeling of sprays using the KIVA code. The publication deals with the problems that are confronted in near nozzle modeling of diesel sprays. Especially sensitivity of atomization modeling to the near nozzle conditions are noted. This publication forms a starting point to Publications II-VII in the sense that the paper gives as a motivation to build a spray model where some of the fundamental phenomena of sprays could be effectively studied.

Publication II deals with turbulence production and dissipation in monodisperse sprays. The paper shows that droplet size could play a crucial role to the formation of large scale vortex structures and turbulence levels in the spray. In single phase jets a ring vortex may be seen in the tip of the jet which is a result of growth of the Kelvin-Helmholtz instability. Here a similar type of vortex ring is seen since the large droplets do not prevent growth of the instability in the considered range of particle loading ratios $\varphi = 0.05 - 0.1$. In the presence of large amounts of small droplets the growth of the instability was noted to be depressed. This effect is demonstrated for two droplet sizes and higher mass-loading ratio of $\varphi = 1.3$. Furthermore, two different spray cloud shapes are observed: in the presence of large droplets a 'mushroom' shaped cloud may be observed whereas small droplets produce a more uniformly dispersed 'fog-like' cloud. The observed tip vortex is characteristic to single phase jets, and it forms due to early times of jet entrainment into the quiescent air. The tip vortex was not observed if the droplets were small due to strong two-way interactions which inhibit the vortex formation process. However, the tip vortex has a strong role to the mushroom cloud shape and the dispersion of

the large droplets. When the tip vortex ring breaks at a certain downstream point, also the large particles become more dispersed. It is speculated that in a general polydisperse spray, the whole spray cloud would form as a superposition of clouds composed of *small* droplets and clouds composed of *large* droplets.

Publication III deals with mixing of passive scalar in a spray and formation of spray cloud dynamics. The publication confirms that, indeed, the spray forms as a superposition of clouds of droplets of different size which is confirmed for sprays having Rosin-Rammler distributed parcel diameters. By changing the SMD of the size distribution it is then possible to emphasize different cloud shape. It is noted that the small droplets disperse in a more uniform way than the large ones. Hence the large drops stay mostly in the center of the jet. The paper implies that in comparison to a single phase jet the particle laden jet spreads more and offers a better mixing. However, in contrast to the preliminary expectations, in the simulated cases no drastic differences in mixing of the passive scalar were observed when the droplet size was varied. This could be partly due to the fact that the passive scalar is released uniformly from the inlet region which might shadow the interpretation of the results. However, the spray shapes were noted to be again rather different which suggests that, instead of passive scalar mixing, it might be a better idea to focus on mixing of the droplets.

Publication IV deals with analysis of spray momentum source term and aims at deeper understanding on the spray mixing process. It is first recognized that the shape of the spray cloud is quite strongly dependent on the particle size. Apparently, if two spray clouds with differing SMD are fundamentally different in shape this can only be possible if the statistical properties of the spray momentum source terms in the Navier-Stokes equation are somehow different. As the momentum source depends on the particle to gas slip velocity it is interesting to study its behaviour. The paper shows that the probability density functions of axial and radial droplet-gas slip velocities depend clearly on the droplet size in such a way that large droplets

have large slip velocities on average as their Stokes number is large whereas small droplets have small Stokes number and thereby they adapt quickly to the local flow conditions. It is also noted that the spatial spray mass distribution depends strongly on the droplet size. Furthermore, the Publication considers the validity of the gradient diffusion model (GDM) which is often used in RANS and LES simulations to model turbulent diffusion of a scalar. In the GDM it is assumed that the turbulent diffusivity is a positive quantity. However, the present results imply that if the actual quantity, that is usually modeled, is explicitely computed, it is seen that the turbulent diffusivity may also be negative. In specific, this happens in the shear layer vortices of the jet. Thus, the results imply that the GD-assumption might be invalid in free shear flows which makes diffusion models based on the GD-assumption doubtful.

Publication V is related to studying the effect of droplet size and breakup on spray shape. To model the droplet breakup a new breakup model is created which is based on the Poisson process. The model is claimed to be simple, yet, it can be used to delay droplet breakup and to control the spray shape. By direct investigation of droplet-wise velocity and slip velocity spectra, the paper shows that large droplets move more independently than the small droplets from the carrier-phase motions. The paper also investigates mixing properties of different droplet sizes using similar methods as in Publication VI and VII. The paper shows some caveats of the present-day droplet breakup models. Namely, droplet breakup in turbulent flows might considerably differ from breakup in laminar flow where droplets with $We < 13$ are usually considered to be stable.

Publication VI is related to carefully studying the effect of Stokes number to the spray shape in the regime $0.07 \leq St_p \leq 2.56$ in monodisperse sprays. For comparison, also polydisperse sprays and a single phase jet with tracer particles is studied. A novel, yet easily implementable, spray visualization algorithm is introduced in the paper. Spray cloud shapes are studied and differences in them explained by

considering the statistical properties of the whole droplet cloud. In specific the probability density functions of the axial and radial components of droplet-gas slip velocity explains the visual observations on the spray clouds.

Publication VII presents an analysis on the effect of droplet size on mixing. In specific the internal structure of the spray clouds is visualized and the structure is noted to be dependent on droplet size. The mixture formation problem is approached in various ways. An important first step is to label all the droplets according to the time the droplet was injected from which droplet residence time (DRT) in the chamber can be easily computed. Hence, the evolution of spray parts is studied and the mixing process can be visualized. The visualization approach clearly shows that droplet size strongly influences mixing in such a way that small droplets may mix much better than the large droplets. The differences in mixing can be clearly characterized and reasoned e.g. from the probability density function (PDF) of local standard deviation of DRT and also remarkably well using its average value. The mixing process is also quantified in terms of droplet diffusivity that depends strongly on droplet size. In fact, the proposed quantitative mixing indicators might be one of the first quantitative measures of fuel spray mixing.

4.2 Summary of the Simulated Cases

Publication I forms an important starting point to the Publications II-VII since the progression of Publications shows what LES has to offer regarding the conventional methods that are used currently in the engineering sector. The Publications II-VII contain the main results of this thesis and a brief summary of the investigated simulation parameters is given in the Tables (4.1)-(4.5). The Tables indicate that monodisperse (i.e. single size parcels) and polydisperse (i.e. parcel size distribution) sprays have been studied. It is also seen that the particle to fluid volume fractions, average Stokes numbers and an estimated average particle to gas mass-loading ra-

tio of the incoming multiphase gas stream. 'Small' mass-loading corresponds to a simulation where a single phase jet is studied with a negligible amount of tracer particles for a reference case. In all the simulations the base flow is the gaseous jet characterized by Reynolds number $Re = 10^4$ and Mach number $Ma = 0.3$. The gas jet velocity is $U_o = 80$m/s with a 5% velocity fluctuation in the axial component. In Publications II-IV the first order implicit Euler time integration scheme is used whereas the second order backward scheme is applied in Publications V-VII. More details on the simulations are given in Publications I-VII.

Table 4.1: Simulated cases in Publication II. Studies using monodisperse sprays ($U_{inj} = 110m/s, \tau_{inj} = 1.0ms$).

diameter	φ	distribution	V_p/V_g	St_p
$2.0\mu m$	1.3	monodisp.	0.007	0.07
$4.0\mu m$	1.3	monodisp.	0.007	0.28
$20.0\mu m$	0.1	monodisp.	0.0005	7
$30.0\mu m$	0.05	monodisp.	0.0003	16
$40.0\mu m$	0.05	monodisp.	0.0003	28

Table 4.2: Simulated cases in Publication III. Studies using polydisperse sprays with Rosin-Rammler distribution varying the SMD. The droplet size range is between 2-40μm. ($U_{inj} = 100m/s, \tau_{inj} = 1.5ms$).

diameter/SMD	φ	distribution	V_p/V_g	St_p
$10.0\mu m$	0.15	polydisp.	0.00075	1.8
$15.0\mu m$	0.15	polydisp.	0.00075	4.0
$25.0\mu m$	0.15	polydisp.	0.00075	11.0
$30.0\mu m$	0.15	polydisp.	0.00075	16.0
$10.0\mu m$	0.3	polydisp.	0.0015	1.8
$15.0\mu m$	0.3	polydisp.	0.0015	4.0
$25.0\mu m$	0.3	polydisp.	0.0015	11.0
$30.0\mu m$	0.3	polydisp.	0.0015	16.0
$2.0\mu m$	small	monodisp.	small	0.07

Table 4.3: Simulated cases in Publication IV. Studies using polydisperse sprays with Rosin-Rammler distribution varying the SMD. The droplet size range is between 2-40μm. Some monodisperse sprays are also considered. ($U_{inj} = 100m/s, \tau_{inj} = 1.5ms$).

diameter/SMD	φ	distribution	V_p/V_g	St_p
2.0μm	0.3	monodisp.	0.0015	0.1
3.5μm	0.3	polydisp.	0.0015	0.25
7.0μm	0.3	polydisp.	0.0015	1
10.0μm	0.3	polydisp.	0.0015	2
2.0μm	0.6	monodisp.	0.003	0.1
3.5μm	0.6	polydisp.	0.003	0.25
7.0μm	0.6	polydisp.	0.003	1
10.0μm	0.6	polydisp.	0.003	2
2.0μm	small	monodisp.	small	0.1

Table 4.4: Simulated cases in Publication V. Studies using monodisperse sprays and polydisperse sprays with the new atomization model. The atomizing droplets start from the nozzle and are initially of size 12μm. Droplets of size 2μm are assumed to be stable. ($U_{inj} = 140m/s, \tau_{inj} = 1.5ms$).

diameter	φ	characterization	V_p/V_g	St_p
2.0μm	0.1	monodisp./non-atom.	0.0005	0.07
5.0μm	0.1	monodisp./non-atom.	0.0005	0.44
12.0μm	0.1	monodisp./non-atom.	0.0005	2.56
12.0 $\rightarrow$ 2μm	0.1	polydisp./fast atom.	0.0005	2.56$\rightarrow$0.07
12.0 $\rightarrow$ 2μm	0.1	polydisp./slow atom.	0.0005	2.56$\rightarrow$0.07

Table 4.5: Simulated cases in Publications VI and VII. Studies using monodisperse sprays and polydisperse sprays with uniform parcel size distribution. ($U_{inj} = 100m/s, \tau_{inj} = 1.5ms$).

diameter	φ	distribution	V_p/V_g	St_p
$2.0\mu m$	0.3	monodisp.	0.0015	0.07
$3.0\mu m$	0.3	monodisp.	0.0015	0.16
$4.0\mu m$	0.3	monodisp.	0.0015	0.28
$5.0\mu m$	0.3	monodisp.	0.0015	0.44
$6.0\mu m$	0.3	monodisp.	0.0015	0.64
$7.0\mu m$	0.3	monodisp.	0.0015	0.87
$8.0\mu m$	0.3	monodisp.	0.0015	1.14
$10.0\mu m$	0.3	monodisp.	0.0015	1.78
$12.0\mu m$	0.3	monodisp.	0.0015	2.56
2.0-$7.0\mu m$	0.3	polydisp.	0.0015	0.07-0.87
2.0-$12.0\mu m$	0.3	polydisp.	0.0015	0.07-2.56
2.0-$17.0\mu m$	0.3	polydisp.	0.0015	0.07-5.13
$2.0\mu m$	small	monodisp.	small	0.07

5 Synopsis

5.1 What Was Done and Why?

The Preliminary Study and Identification of the Problem: Spray mixing and combustion is a strongly transient process where the instantaneous turbulence characteristics have a major effect to the spray structure and emissions [6, 15, 18, 57, 97]. When the LES part of this work started in 2006, it was clear that the state-of-the-art RANS-models are not able to reproduce the temporal and spatial spray characteristics as seen in experiments. For example, during preparation of Publication I in 2006 it became clear that there is apparently 'something lacking' in the simulations. The first numerical experiment, in which spray simulations with RANS and LES turbulence models was compared, was carried out by Hori et al. in the work from 2006 [30]. The results showed that LES captures the transient features and eddy structure of the flow because the grid scale turbulence is directly solved and only the subgrid scale turbulence is modeled. The RANS approach assumes that all the turbulent scales are isotropic, and hence the method can not be used to reproduce the spatio-temporal correlations such as local mixture inhomogeneities that are formed also due the larger turbulent structures. In RANS modeling one has to also resort to a dispersion model in order to simulate the random shape of a spray. Also in LES a dispersion model is needed if a large proportion of the SGS kinetic energy is modeled. Thus, LES was considered to be the necessary step 1) to create spray pictures that are realistic from spatio-temporal viewpoint because in (implicit) LES the energy containing scales are resolved, and 2) to simulate the effect of droplet size on mixture inhomogeneities.

The Main Study and Application of LES to Solve the Problem: From the experiences of Publication I it became clear that the near nozzle region is nu-

merically and physically problematic. In specific, the LES/LPT approach becomes inconsistent in the near nozzle region when the grid spacing is refined to the LES resolution. As particle laden jets had been in studied in various setups by several authors using LES [31]-[42] and by experiments [43]-[45] a decision was made to use the droplet laden jet as a test case. This setup would 'emulate' the spray behavior in the dilute regions far from an injector and the near-nozzle regime would be avoided. The first idea was to study droplet originated turbulence production and dissipation in Publication II. Although production and dissipation differences were observed, most importantly, the experiences from Publication II showed the extreme differences between the dispersion patterns of small and large droplets together with the flow structures. A decision was then made to carefully investigate droplet size effects to dispersion and study the mixing problem in Publications III-VII. The mixing was first approached by investigating passive scalar mixing in the turbulent fields. However, it was noted that the results might be somewhat difficult to interpret in terms of droplet size and other means needed to be considered. The key to understand the mixing better was found in Publication IV in which it was shown that the slip velocity of the small droplets is typically small and its PDF is concentrated to small values as well. The progression of studies in Publications V-VII then carefully show that the mixing can be understood quantitatively by labeling all the droplets and then analyzing how much the initial starting configuration of the droplets changes. The approach is mathematically rigorous and tells consistently the mixture quality. Thus, in Publications V-VII mixing was viewed as growth of disorder in the system.

5.2 Why Were Spray Sub-Models Not Used?

Modeling Complications: It is commonly known that CFD-spray modeling is a very complex task and that there are many uncertainities in the models [25]. Further complications arise since most of the existing spray sub-models have been tailored originally for the RANS-context and it is not clear how to apply such models

in the LES context. Not only this but the combination of a turbulence modeling approach (RANS) and spray submodels may lead to conclusions that depend on the modeling combination and are not necessarily of physical origin [25]. Finally, the parcel approach gives extra complications since it is not clear that applying a certain model of e.g. droplet evaporation, breakup etc. to all droplets in a parcel in a deterministic way gives the desired result. Thus, the spray sub-models include several components that cause uncertainities to the results and hence a decision was made to considerably simplify the situation by switching the submodels off.

Turbulence-Originated Droplet Dispersion of Primary Interest: A physical phenomenon of primary importance in sprays is droplet dispersion. Several physical phenomena may play role in formation of a dispersion. 1) The inner nozzle effects such as cavitation may affect the spray opening angle which apparently has an effect on the initial direction that the largest droplets move from the nozzle [1, 7, 25]. 2) Droplet breakup is important from the viewpoint of dispersion because after the breakup the smaller the droplets are the more they are dispersed by the turbulent gas motions. 3) Droplet collision should be important from the viewpoint of dispersion since collisions redistribute momentum and energy to random directions. 4) Spray opening angle might be important to the fuel jet characteristics. However, if none of the above-mentioned phenomena are modeled/taken into account, the turbulent gas motions alone are responsible for causing the spray to disperse. One of the main missions in the thesis was to show that in LES, if properly applied, it is possible to simulate a realistic spray without any other models than the droplet equation of motion.

5.3 Places for Improvement

5.3.1 Numerical Methods

Spatial Accuracy: High quality LES requires that the spatial derivatives are discretized with a discretization method that is at least second order accurate in space. On unstructured grids this is usually also the highest achievable accuracy in practice. Hence, the non-dissipative second order accurate central difference scheme together with a high spatial grid resolution is likely to be one of the best schemes for carrying out LES in practice if one adds artificial dissipation that keeps the simulation algorithm numerically stable. In specific, when studying the two-way coupling problem using the LPT method one makes several simplifications on the particle phase. For example, the parcel concept is a rather coarse description of the reality. Hence, one may argue that unless the LPT approach is improved considerably (by e.g. resolving the motion of all droplets) there is probably no reason to increase the order of spatial discretization but more likely to increase the number of parcels and refine the mesh. Nevertheless, there are several higher order accurate spatial discretization methods that have become quite popular recently such as the WENO (Weighted Essentially Non-Oscillatory) method [52, 66] or the third order accurate upwind-method [22, 48, 49]. In compressible flows at rather high Mach numbers especially the WENO method has proved out to be rather robust in the sense of e.g. capturing shocks. If one is interested in simulating particle dispersion, probably any of the higher order schemes will work as long as the scheme resolves a high enough range of frequencies. Yet, it is well known that the higher order schemes may develop non-physical oscillations to the solution which might be undesirable. If the problem of two-way coupling is studied in detail one probably needs to use a non-dissipative central scheme to avoid any coupling between numerical diffusion and the actual momentum source term. In this way the numerical errors are not accumulated.

Temporal Accuracy: Nowadays the explicit Runge-Kutta (RK) family of time-integration schemes have become very popular in the simulation of turbulent flows [22, 46, 48, 49, 50, 88]. The RK-schemes provide a high temporal accuracy and they are also computationally rather moderate since explicit low-storage schemes do not require the solution of an algebraic group of equations. The advantage of explicit schemes is also the causal nature of turbulent flows: the solution in the future depends only on the current state of the system and hence explicit schemes can be reasoned to be, not only computationally efficient, but also logical choice in the simulation of turbulent flows. The disadvantage of explicit schemes is the timestep restrictions which, however, needs to be rather small in LES anyways. RK-schemes can also be easily implemented to the OpenFOAM code which would be a logical next step to proceed to further improve the quality of these simulation results.

Solution of a Linear System of Equations: OpenFOAM provides the user with several options for the solution of symmetric and asymmetric systems of equations. In the present work an Incomplete Cholesky (Bi-)Preconditioned Conjugate Gradient (ICPCG) method was applied to the solution of asymmetric and the ICP(B)CG method for the solution of symmetric groups of equations. However, the Multigrid methods have become increasingly popular and effective approach to the solution of the pressure equation [22]. The MG-method has the algorithmic complexity of $\mathcal{O}(N \log N)$ with the number of grid points which is comparable in efficiency to the optimized complexity of the Fast-Fourier Transform that is used in the context of pseudo-spectral methods [88].

5.3.2 Lagrangian Particle Tracking

The LPT approach could be much improved if all the droplets would be resolved. From the physical viewpoint, this would give an improved basis for using CFD submodels for e.g. droplet breakup, inter-droplet collision and inter-droplet drag

reduction. From the numerical viewpoint the stability of numerical algorithms would be improved by making the momentum source more spatially dispersed since an individual droplet carries less momentum than a parcel. If the droplets are large (but much smaller than the cell size) there are basically rather few problems since all the droplets can be resolved. However, if the droplets are small, many droplets need to be gathered into a parcel. At least two solutions can be outlined. 1) One could formulate a continuum approach for droplet number density together with the Eulerian droplet velocity field. 2) One could simply 'accept' to live with the parcel approach i.e. the finite number of parcels but, instead of only nearest-neighbour parcel-gaseous phase cell interactions, one could also resort to those cells that are further away. Distributing momentum between a larger number of cells would also lead to an enhanced numerical stability.

5.3.3 Mesh Issues

Simulation of transitional flows is challenging due to several reasons. For example, 1) the details of the transition process may be mesh dependent i.e. the mesh may trigger a certain instability mode, and 2) the simulation of the turbulence transition process requires a fine resolution which makes it computationally expensive. For example, in this work the mesh needed to be stretched in the streamwise direction to make it finer near the inlet and coarsen it gradually. The mesh needed to be also stretched in the radial direction. An even better way to create a mesh for the current setup would be to make the mesh uniformly spaced in streamwise and radial directions until e.g. $z/D < 20$ and $r/D < 2$. The stretching would be admitted outside the uniform region. This would provide a better numerical accuracy. Improved numerical accuracy could also be obtained by using a Cartesian mesh in the important parts of the flow where the determining physics takes place (e.g. shear layers, boundary layers, high energy density regions etc.). Using a Cartesian mesh would provide also the best numerical accuracy. Yet, using such a mesh in a flow

with a certain symmetry (e.g. round transitional jet) might cause an extra flavour to the solution until the flow is fully developed.

5.3.4 Boundary Conditions

It would be possible to use a turbulent boundary condition at the jet inlet that has been sampled from a precursor simulation. In this way the incoming flow would be readily turbulent. Of course, such a boundary condition gives new degrees of freedom (e.g. assumptions of flow emanating from a pipe) and hence, in the present study, a randomly perturbed laminar top hat inlet profile was chosen due to its simplicity. In nearly incompressible flows, one of the most used outflow boundary conditions is the convective boundary condition [22, 49]. The convective boundary condition assumes that the material derivative $D\mathbf{u}/Dt = 0$ at the outlet if fluid flows out of the domain and the velocity is set to zero if fluid tries to re-enter the domain. In the present study, a zero-gradient condition was used which was found to be good enough if the outlet was far enough from the active flow region. The choice was made because the convective boundary condition had not been implemented to earlier versions of the present simulation code.

5.4 How to Put the Results of This Study Into Practice?

Implications to Injector Development: It was demonstrated that one simple parameter, the fuel droplet size, may influence the air utilization and therof mixing inside the spray by 100%. It is generally believed that small fuel droplets lead to enhanced mixing which can be achieved by decreasing nozzle diameter (to as low as e.g. 100μm) and by increasing the injection pressures to very high levels (e.g. well over 2000bar). Hence, the results of this study support such developments as

this work implies that the mixing (and $\phi-$ distribution) inside the fuel spray can be lowered by decreasing droplet size.

Implications to Numerical Simulations: Numerical simulation and modeling of sprays is and remains a very complicated task. In this study a rather 'reserved' approach towards spray modeling was taken since all the submodels (except of course the equations of motion and Newton's laws) were switched off. The only submodel that was eventually used was the stochastic breakup model developed in Publication V. The following notifications and suggestions are made to CFD spray modelers who work in the field of LES/LPT:

- Spray dispersion forms due to turbulence which is produced especially in the shear layer of the spray. Hence, in order to simulate spray dispersion properly, a significantly higher spatial and temporal resolution is required than is usually applied in e.g. RANS simulations. For example, in this work $\Delta x < 10^{-4}m$ and $\Delta t < 10^{-7}m$.

- Spray dispersion properties are *very* sensitive to droplet size as the Stokes number is proportional to d^2. Hence, for example, it is a highly relevant question to know whether the droplets are e.g. $10\mu m$ or $5\mu m$ in size. Therefore, all the models that influence droplet size should be thoroughly understood. In Publication V critical points of the state-of-the-art droplet breakup models were considered and it was pointed out that droplets with low Weber number ($We < 13$) may potentially break due to resonance interactions. This is in contrast to practically all droplet breakup models that are currently in use in commercial CFD-codes.

5.5 How to Generalize These Results?

Solution of Partial Differential Equations: As always, the results of a study that is related to PDEs depend on 1) the initial conditions and 2) the boundary conditions [87]. Furthermore, all numerical results depend, at least to some extent, on the methods and the grids together with the underlaying modeling assumptions.

Effect of Reynolds Number: This study was carried out at a jet inlet Reynolds number $Re = 10^4$ which is a characteristic order of magnitude in diesel sprays. The behavior of jets at higher Reynolds numbers has been discussed in the literature [8, 48, 90, 91, 95, 100] but the main phenomena seem to remain rather unchanged around this order of magnitude. However, at lower Reynolds numbers (e.g. Re=1000) the jets become less turbulent although they are never stable [99]. Hence, it can be stated that studying the jet at $Re = 10^4$ is a reasonably representative case to study dispersion.

Effect of Gas and Droplet Density: If the gas density would be increased the fluid would become heavier. Correspondingly, the mass-loading φ would decrease which would make the situation closer to one-way coupling. Similarly, also the Stokes number of the droplets would decrease with the inverse of gas density. Thus, increasing the gas density would make also the large droplets to behave like the small droplets and their dispersion would be increased. However, from the numerical viewpoing, one would also need to decrease the timestep from the present case since the motion of the smallest droplets would not be resolved for too small τ_p. Opposite effects would be seen if only the droplet density would be increased and the gas density would stay as a constant. The mass-loading would increase and the two-way coupling would become more pronounced. Also the small particles would start to resemble the large particles.

Effect of Droplet Size: If the droplet size would be increased too much the

droplets would become larger than the grid spacing which would make the simulations inconsistent with the assumptions of LPT. Also the droplet Reynolds number would increase. Physically speaking, when $Re_p > 300$ one should start to take into account the effect of the interactions of the unsteady droplet wake with the turbulent motions [61].

Effect of Inlet Velocity Profile: It is well known that the jet inlet velocity profile is important for the development of the shear layer. For example, Hällqvist [49] showed that a 'mollified' profile may lead to a persistent shear layer and promote the formation of large scale vortex structures. Hence the inlet profile is an important factor in governing also the spray dispersion and it should be further studied.

Effect of Inlet Spray Mass Profile: In order to emulate a real diesel spray in an improved way one could for example choose a radially varying Gaussian mass distribution for the spray at the inlet. Then, one would also need to develop an expression for the corresponding radial velocity distribution for the droplets and the gas.

Effect of Initial Turbulence: The initial turbulence in the chamber would probably have an effect on the appearance of the spray by making the spray more unstable and dispersed. Especially, if the energy density of the initial flow field perturbations is comparable to the energy density of the spray.

Effect of Droplet Drag Law: The droplet equations of motion must be considered to be a model of droplet motion which neglect the presence of other droplets and also the smallest turbulent scales. However, if these simplifications are accepted (as is common) the model is very useful and it has been noted to produce realistic results in terms of velocity correlations by several authors [31, 32, 34, 37]. It is very important to note that the drag law is a non-linear function of the slip velocity. Hence, the droplets also respond non-linearly to the gas motions.

Effect of the Initial Droplet to Gas Slip Velocity: The initial slip velocity is an important factor in determining the dispersion pattern as implied also in the study by Wu and Fuchs [39]. For the large droplets, the larger the initial slip the longer the droplets penetrate and the later downstream their dispersion begins. For the smaller droplets the differences are not as pronounced. Furthermore, it should be noted that the larger the initial slip, the stronger the two-way coupling.

Effect of the Mass-Loading Ratio: The larger the amount of the injected fuel the more the properties of the base flow change. One indication is the prolongation of the potential core as noted in e.g. Publications II-IV. The behavior of the particle laden jet can be 'manipulated' in various ways. For example, loading the jet heavily with small particles having zero initial velocity results in strong absorption of the carrier phase energy. In contrast, loading the jet heavily with large particles and injecting the particles with high velocity will cause different kind of behaviour.

Effect of Spray Opening Angle: For example, in RANS modeling the spray opening angle is usually modeled. In this work, however, the angle was not modeled and it forms purely due to the spreading of the jet. Probably, if the angle would be modeled, this would have some effect. Especially, when the droplets have a large St_p they will propagate to the direction of the initial angle for a rather long time. However, if the droplets have a small St_p the effect of the initial angle should be smaller.

5.6 Sprays in Simplified Conditions: Relevant or Not?

Role of Evaporation: An issue with non-evaporating spray studies is that the connection to 'real-world' evaporating fuel sprays is often not fully understood. However, the following issues should be noted. First, there are engine concepts where spray evaporates slowly which means that the droplet timescale τ_p has relevance for

spray formation in a real situation [3]. Second, in the limit of small τ_p the situation can be related to a vaporizing situation because the small droplets follow the flow similar to the fuel vapor. As non-vaporizing sprays are easier to study it is very useful to understand how a non-vaporizing spray evolves and mixes. Third, it has been pointed out that the instantaneous spray distribution together with droplet size distribution have a primary role for fuel ignition in many applications [97]. This ignition delay (i.e. the time from SOI to the appearence of the flame) can be of the same order of magnitude as the fuel injection duration and hence it also characterizes the time of initial mixture formation which should influence the local levels of ϕ.

Role of Atomization: One might argue that it is not relevant to study sprays without an atomization model. However, the important thing that should noticed is the timescale of atomization. If that timescale is much smaller than the integral timescale of the flow the atomization modeling should not be relevant. Otherwise it might be necessary to model. In modern diesel engines the breakup timescale is small enough so that studying a non-atomizing spray is a good approximation.

Other Issues: In general, emission control is a rather difficult topic and it is not completely clear which of the engine components one should mostly focus at when optimizing the emission levels. For example, one could argue that it is less necessary to focus on the spray since the global emission levels could be better controlled by applying exhaust gas recirculation (EGR). However, this study shows that not only the global but also local value of ϕ [1] might have a strong role on the emissions because e.g. EGR alone does not remove mixture heterogeneities (i.e. preferential concentration) which probably influences the level of emissions (c.f. Fig. 3.14). For example, in this study it is shown that only 50% of the air inside the fuel spray may be utilized if the droplet size is too large. Hence, the present results imply that one needs to be fully aware of spray structure and droplet size distribution in order to fully understand mixture quality prior and during combustion.

5.7 Did This Study Really Contribute to the State-of-the-Art?

A Vast Number of Studies Already Exist: Particle laden jets and particle dispersion have been studied experimentally by several authors [43]-[45]. Large-Eddy Simulation studies on particle laden jets have been previously carried out by various authors [31]-[42]. Particle dispersion and the effect of particle size on the dispersion at various wall-bounded and isotropic suspensions have been studied extensively in the past [69]-[77]. Hence, according to the literature it could be stated that the role of Stokes number on particle dispersion is understood, if not perfectly, then at least satisfactorily. Furthermore, the utilization of sprays in the society and diesel fuel injection systems is anything else but a new topic and, thereof, it is necessary to explain the 'new real contribution' of this study?

Extensive Scope: An important general contribution of the work is the scope of the work itself with respect to many previous studies. The work consists of a preliminary study on the currently existing RANS-based spray models in Publication I. After this it became clear from the literature that LES is needed in order to simulate sprays in a more realistic manner. It also became apparent from the literature that particle/droplet dispersion can be studied using a jet base flow. Then, the main part of the thesis consists of a progression of studies presented in Publications II-VII that have been all carried out on the same setup. Hence this study is rather extensive in contrast to previous, individual works on particle laden flows.

Utilization of LES/LPT, Novel Visualization and Statistical Analysis: Another important general contribution of the work is the systematic use of the method itself (LES) to better understand the effect of droplet size on droplet dispersion. Special attention has been put to investigating the regime $0.1 \leq St_p \leq 3$ which gives the most interesting dynamics for the spray patterns due to timescale interaction between the droplets and the gaseous phase as thoroughly discussed in Publications V-VII. The primary aim was to use the simulation tools to demonstrate that the

same physical phenomena as seen in experiments, can be reproduced in the model problem using LES. In contrast to previous studies, in this work a *transient* spray analysis was presented and it was shown that spray behavior (as a function of Stokes number) can be very coherently explained using such data which is important since e.g. spray combustion depends rather on the instantaneous than time averaged fuel spray properties. In contrast to previous studies, visualization formed the core part of this work and a considerable effort was made to visualize the simulated sprays in a realistic way. Improvements in the visualization are seen throughout the thesis and finally in Publications V-VII the sprays 'look real'. The Author is not aware of any previous simulation studies in which one could not immediately tell the difference between a 'simulated spray' and an 'experimental spray'. Often especially transient visualization is considered to be a rather subjective means of analysis of results and thus it is sometimes even omitted from the data analysis. Importantly, here the visualization was combined with statistical analysis of instantaneous droplet cloud data (droplet velocities, coordinates etc.) and quantitative means to analyze mixing were developed. This kind of analysis can hardly ever be done with experimental methods and LES/DNS is needed to handle the task. The Author is not aware of previous such attempts.

The Challenging Physics of Diesel Sprays: In a rather recent review by Smallwood and Gülder [7] it has turned out that the previously existing picture on the physics of sprays might be inadequate and that further investigations are needed. For example, the existence of a long intact liquid core, that was previously stated to extend as long as $100d_n$ from the nozzle, has turned out to be somewhat misleading since several authors have noted that the spray is completely atomized near the nozzle exit within a few nozzle diameters. The work done in Publication I supports the latter view because the core was noted to be fragmented reasonably fast already at low densities which implies that the fragmentation is significantly stronger at realistic engine operating conditions. Subsequently, especially in modern engines with high pressure fuel injection, the role of secondary droplet breakup has turned

out to be much less important (or at least not to extend as long downstream as in older engines) than has been previously thought (see [7] and the citations therein). Apparently, if this is the case, it could be possible in certain cases to simply ignore the droplet breakup models from numerical simulations of diesel sprays which would significantly simplify the task of engine spray modelers. In Publication V droplet breakup modeling was considered and new aspects on the breakup process modeling were developed. In specific, the low Weber number breakup was investigated which is in contrast to the high Weber numbers that have been previously assumed. The low Weber number breakup can also be related to the afore-mentioned observations on the changes of views on the secondary breakup process. Hence, quite drastic changes in the views on the physics of sprays have been recently discovered, both due to 1) improved experimental techniques, and 2) higher fuel injection pressures in modern engines which have not been so extensively studied yet. Thus it is necessary to look at the basic phenomena in sprays thoroughly. That is why in this study spray submodels were switched off in order to look at the effect of Stokes number on spray dispersion as such.

6 Conclusions and Outlook

Conclusions: An analysis regarding the effect of droplet size on spray formation has been presented. The following conclusions were made:

- The used simulation method produces a realistic spray shape and captures the known features on the effect of St_p on droplet dispersion.

- Large droplets follow the low frequency motions of the fluid. Small droplets follow also the high frequency motions of the fluid and hence their temporal frequency response is much higher. This can be seen from droplet velocity and slip velocity PDFs and from the spectra of individual droplet time-series which together complete the picture and, on their side, explain the differences in spray shapes.

- In the present setup the small droplets were noted to mix much better than the large droplets. Three reasons for this are suggested: 1) The small droplets respond to the motion of the turbulent fluctuations very quickly and hence the 'mixing potential' of the turbulent jet is realized efficiently. 2) The amount of the small droplets is reasonably small so they do not excessively dissipate the turbulent fluctuations. 3) The present base flow does not exhibit a very persistent shear layer which could considerably delay the turbulence transition process and affect the mixing process.

- Two new quantitative mixing indicators have been suggested in Publications V and VII which both depend strongly on St_p and they explain the spray shapes.

- Spray tip has a strong effect on the dispersion of large droplets and complex, non-linear interactions arise due to the tip effects.

- The literature implies that droplet breakup modeling in low Weber number flows might also be important. The *a priori* simulations in Publication V imply that modeling this effect in CFD simulations might be highly important since the phenomenon has potentially very strong consequences to the level of mixing.

Outlook: A topic for future study would be to model the spray jet boundary conditions so that they would be closer matched with experiments. This could be done by e.g. choosing a Gaussian mass distribution profile for the spray mass at the inlet. Consequently, the gas and droplet velocity distributions at the inlet would need to be specified because apparently the profiles must be closely correlated. In general, these modifications would be likely to affect the development of the spray shear layer and thereby one might observe some differences in the vortex structures in comparison to the present top hat profile. Also the jet inlet could be made more narrow in order to minimize the influence of the boundary condition to the spray development. In diesel-engines the turbulence levels and the in-cylinder flow structures will also influence the spray behavior. Thus, it is rather challenging to give unique guidelines for future LES/LPT development since different engine applications might require focusing on different topics. However, a future topic that is closely related to many types of spray problems is the mixing of two miscible fluids with different densities. Of specific interest would be the injection of a fuel jet of species 1 with density ρ_1 into the ambient gas of species 2 with another density ρ_2. Namely, this problem is very closely related to quickly evaporating fuel sprays (such as in conventional DI diesel engines) and sprays with very small droplets (such as in modern DI HCCI engines). The influence of the inflow boundary condition has a great role there as well. Simulation of such a mixing problem with LES would be a challenging but also a meaningful task, even at high density ratios, because one avoids many modeling complications and uncertainities that are associated with LPT at high liquid fuel to air volume fractions. Our future research focuses on LES of DI gas engines where mixing of a methane jet with air is of interest.

References

[1] Heywood J., Internal Combustion Engine Fundamentals, McGraw-Hill, ISBN-0-07-100499-8, (1989).

[2] Dec J.E., *A Conceptual Model of DI Diesel Combustion Based on Laser-Sheet Imaging*, SAE Technical Paper Series 1997-970873, (1996).

[3] Wahlström J., *Low Temperature Combustion - Combustion Process, Control Methods and Fuels*, Publications of the Internal Combustion Engine Laboratory, Helsinki University of Technology 83, ISSN-1459-5981, (2007).

[4] Akihama K., Takatori Y., Inagaki K., Sasaki S. and Dean A.M., *Mechanism of the Smokeless Rich Diesel Combustion by Reducing Temperature*, SAE Technical Paper Series 2001-01-0655, (2001).

[5] Siebers S. and Higgins B., Flame Lift-Off on Direct-Injection Diesel Sprays Under Quiescent Conditions, SAE Technical Paper Series 2001-01-0530, (2001).

[6] Pickett L.M. & Siebers D.L., *Orifice Diameter Effects on Diesel Fuel Jet Flame Structure*, Journal of Engineering for Gas Turbines and Power, **127**, (2005).

[7] Smallwood G. & Gülder, *Views on the Structure of Transient Sprays*, Atomization and Sprays, **10**, 355-386, (2000).

[8] Pope S.B., *Turbulent Flows*, Cambridge University Press, ISBN 0-521-59886-9, (2001).

[9] Lefebre, A.H., *Atomization and Sprays*, Hemisphere Publishing Corporation, (1989).

[10] Faeth G.M., *Spray Combustion Phenomena*, Twenty-Sixth Symposium on Combustion/The Combustion Institute, 1593-1612, (1996).

[11] Naber J.D. and Siebers D.L., *Effects of Gas Density and Vaporization on Penetration and Dispersion of Diesel Sprays*, SAE Technical Paper Series 1996-960034, (1996).

[12] Cao Z.M., Nishino K., Mizuno S., and Torii K., *PIV Measurement of Internal Structure of Diesel Fuel Spray*, Experiments in Fluids, 211-219, (2000).

[13] di Stasio S., Valentino G. and Corcione F.E., *Spray Boundary Concept and Droplet Size Distribution of Dense Diesel Jets by Different Laser Experiments*, in the Proceedings of 16th Annual Conference on Liquid Atomization and Spray Systems, ILASS Europe-2000 (2000).

[14] Stegemann J., Seebode J., Baltes J., Baumgarten J. and Merker G.P., *Influence of Throttle Effects at the Needle Seat on the Spray Systems*, in the Proceedings of 18th Annual Conference on Liquid Atomization and Spray Systems, ILASS Europe-2002 (2002).

[15] Ganippa L.C., *Atomisation and Combustion Studies of Diesel Sprays*, PhD Thesis, Göteborg, Sweden, ISBN-91-7291-326-6, (2003).

[16] Wahlin F., *Experimental Investigations of Impinging Diesel Sprays for HCCI Combustion*, PhD Thesis, KTH, Stockholm, ISSN-1400-1179, (2007).

[17] Roisman I.V., Araneo K. and Tropea C., *Effect of Ambient Pressure on Penetration of a Diesel Spray*, Int. J. Multiphase Flow, **33**, 904-920, (2007).

[18] Hillamo H., Kaario O. and Larmi M., *Particle Image Velocimetry Measurements of a Diesel Spray*, SAE Technical Paper Series 2008-01-0942, (2008).

[19] Fureby C., Tabor G., Weller G. and Gosman A.D., *A Comparative Study of Subgrid Scale Models in Homogeneous Isotropic Turbulence*, Phys. Fluids, **9**, 1416-1428, (1997).

[20] Grinstein F.F., Fureby C. and DeVore C.R., *On MILES Based on Flux-Limiting Algorithms*, Int.J.Numer.Meth.Fluids, **47**, 1043-1051, (2005).

[21] Grinstein F.F. and Fureby C., *Recent Progress on Flux-Limiting Based Implicit Large Eddy Simulation*, European Conference on Computational Fluid Dynamics, ECCOMAS CFD 2006, (2006).

[22] Ferziger J.H. and Perić M., *Computational Methods for Fluid Dynamics*, Springer, ISBN 3-540-65373-2, (1999).

[23] Tannehill J.C., Anderson D.A. and Pletcher R.H., *Computational Fluid Mechanics and Heat Transfer*, Taylor&Francis, ISBN-1-56032-046-X, (1997).

[24] Tanner F.X., *Development and Validation of a Cascade Atomization and Drop Breakup Model for High-Velocity Dense Sprays*, Atomization and Sprays, **14**, 1-27, (2004).

[25] Stiesch G., *Modeling Engine Spray and Combustion Processes*, Springer, ISBN 3-540-00682-6, (2003).

[26] Amsden A.A., O'Rourke P.J. and Butler T.D., *KIVA-II: A Computer Program for Chemically Reactive Flows with Sprays*, Technical Report LA-11560-MS, Los Alamos National Laboratory, (1989).

[27] Rüger M., Hohmann S., Sommerfeld M. and Kohnen G., *Euler/Lagrange Calculations of Turbulent Sprays: the Effect of Droplet Collisions and Coalescence*, Atomization and Sprays, **10**, 47-81, (2000).

[28] Kärrholm, F.P., Numerical Modelling of Diesel Spray Injection, Turbulence Interaction and Combustion, PhD thesis, Chalmers University of Technology, Göteborg, (2008).

[29] Kärrholm F.O. and Nordin N., Three-Dimensional Simulation of Diesel Spray Ignition and Flame Lift-Off Using OpenFOAM and KIVA-3V CFD Codes, SAE Technical Paper Series 2008-01-0961, (2008).

[30] Hori T., Senda J., Kuge T. and Fujimoto H., *Large Eddy Simulation of Non-Evaporative and Evaporative Diesel Spray in Constant Volume Vessel by Use of KIVALES*, SAE Technical Paper Series 2006-01-3334, (2006).

[31] Apte S., Gorokhovski M. and Moin P., *LES of Atomizing Spray with Stochastic Modeling of Secondary Breakup*, Int. J. Multiphase Flow, **29**, 1503-1522, (2003).

[32] Apte S., Mahesh K., Moin P. and Oefelein J.C., *Large-Eddy Simulation of Swirling Particle-Laden Flows in a Coaxial-Jet Combustor*, Int. J. Multiphase Flow, **29**, 1311-1331, (2003).

[33] Ham F., Apte S., Iaccarino G., Wu X., Herrmann M., Constantinescu G., Mahesh K. and Moin P., *Unstructured LES of Reacting Multiphase Flows in Realistic Gas Turbine Combustors*, Annual Research Briefs 2003, Center for Turbulence Research, University of Minnesota, pp. 139-160, (2003).

[34] Sankaran V. and Menon S., *LES of Spray Combustion in Swirling Flows*, Journal of Turbulence, **3**, (2002).

[35] Pitsch H., *Large-Eddy Simulation of Turbulent Combustion*, Annu. Rev. Fluid Mech., **38**, 453-82, (2006).

[36] Lieuwen T. & Yang V., *Combustion Instabilities in Gas Turbine Engines: Operational Experience, Fundamental Mechanisms and Modeling*, **210**, Progress in Astronautics and Aeronautics, ISBN 1-56347-669-X, (2005).

[37] Oefelein J.C., Sankaran V. and Drozda T.G. Large Eddy Simulation of Swirling Particle-Laden Flows in a Model Axisymmetric Combustor, Proceedings of the Combustion Institute, **31**, 2291-2299, (2007).

[38] Bini M. and Jones W.P., Large Eddy Simulation of an Evaporating Acetone Spray, Int. J. of Heat and Fluid Flow, **30**, 471-480, (2009).

[39] Wu Z. and Fuchs L., *Large Eddy Simulation of Dispersion of Particles in Turbulent Jets*, Journal of Computational and Applied Mechanics, **2**, 21-35, (2001).

[40] Luo K., Klein M., Fan J.-R. and Cen K.-F., *Effects on Particle Dispersion by Turbulent Transition in a Jet*, Physical Letters A, **357**, 345-350, (2006).

[41] Ling W., Chung J., Troutt T. & Crowe C., *Direct Numerical Simulation of a Three Dimensional Temporal Mixing Layer with Particle Dispersion*, J. Fluid Mech., **358**, 61-85, (1998).

[42] Yan J., Luo K., Fan J., Tsuji Y. and Cen K., *Direct Numerical Simulation of Particle Dispersion in a Turbulent Jet Considering Inter-Particle Collisions*, Int. J. Multiphase Flow, **34**, 723-733, (2008).

[43] Longmire E.K. and Eaton J., *Structure of a Particle-Laden Round Jet*, J.Fluid Mech., **236**, 217-257, (1992).

[44] Chen Y.C., Starner S.H. and Masri A.R. A Detailed Experimental Investigation of Well-Defined, Turbulent Evaporating Spray Jets of Acetone, Int. J. Multiphase Flow, **32**, 389-412, (2006).

[45] Ferrand V., Bazile R., Borée J. and Charnay G., *Gas-Droplet Turbulent Velocity Correlations and Two-Phase Interaction in an Axisymmetric Jet Laden with Partly Responsive Droplets*, Int. J. Multiphase Flow, **29**, 195-217, (2003).

[46] Grinstein F.F., Margolin L.G. and Rider W.J., *Implicit Large Eddy Simulation*, Cambridge University Press, ISBN 978-0-521-86982-9, (2007).

[47] Caraeni D.A., *Development of a Multidimensional Residual Distribution Solver for Large Eddy Simulation of Industrial Turbulent Flows*, Doctoral Thesis, ISBN-91-628-4280-3, (2000).

[48] Olsson M. and Fuchs L., *Large Eddy Simulation of the Proximal Region of a Spatially Developing Circular Jet*, Phys. Fluids, **8**, 2125-2137, (1996).

[49] Hällqvist, T., *Large Eddy Simulation of Impinging Jets with Heat Transfer*, PhD thesis, KTH, Stockholm, (2006).

[50] Berglund M., *Large-Eddy Simulation of Complex Turbulent Flows*, PhD Thesis, Lund, Sweden, ISBN-978-91-628-6879-6, (2006).

[51] Salewski M., *LES of Jets and Sprays Injected into Crossflow*, Doctoral Thesis, ISBN-13-978-91-628-6967-0, (2006).

[52] Salewski M. and Fuchs L., *Consistency Issues of Lagrangian Particle Tracking Applied to a Spray Jet in Crossflow*, Int. J. Multiphase Flow, **33**, 394-410, (2007).

[53] Brennen C., *Fundamentals of Multiphase Flow*, Cambridge University Press, ISBN-13 978-0-521-84804-6, (2005).

[54] Crowe C.T., Sommerfeld M. and Tsuji Y., *Multiphase Flows with Droplets and Particles*, CRC Press, (1998).

[55] Kolmogorov A.N., *On the Drop Breakup in Turbulent Flows*, Gidromekanika, DAN LXVI (NS), 825-828, (1949).

[56] Brown W.K. and Wohletz K.H., *Derivation of the Weibull Distribution Based on Physical Principles and its Connection to the Rosin-Rammler and Lognormal Distributions*, J.Appl.Phys. **78**, 2758-2763, (1995).

[57] Cao J., *On the Theoretical Prediction of Fuel Droplet Size Distribution in Nonreactive Diesel Sprays*, Journal of Fluids Engineering, **124**, 182-185, (2002).

[58] Hsiang L.P. and Faeth G.M., *Drop Deformation and Breakup Due to Shock Wave and Steady Disturbances*, Int.J. Multiphase Flow, **21**, 4, pp. 545-560, (1995).

[59] Hsiang L.P. and Faeth G.M., *Temporal Properties of Secondary Drop Breakup in the Bag Breakup Regime*, Int.J. Multiphase Flow, **24**, pp. 889-912, (1998).

[60] Dai Z. and Faeth G.M., *Temporal Properties of Drop Breakup in the Multimode Breakup Regime*, Int.J. Multiphase Flow, **27**, pp. 217-236, (2001).

[61] Mittal R., *Response of the Sphere Wake to Freestream Fluctuations*, Theoret. and Comput. Fluid Dynamics, **13**, 397-419, (2000).

[62] Martinez-Bazán C., Montañes J.L. and Lasheras J.C., *Bubble Size Distribution Resulting from the Breakup of an Air Cavity Injected into a Turbulent Water Jet*, Physics of Fluids, **12**, 1, 145-148, (2000).

[63] Lasheras J.C., Eastwood C., Martínez-Bazán and Montañés, *A Review of Statistical Models for the Break-up of an Immiscible Fluid Immersed into a Fully Developed Turbulent Flow*, Int.J. Multiphase Flow, **28**, pp. 247-278, (2002).

[64] Pilch M. and Erdman C.A., *Use of Breakup Time Data and Velocity History Data to Predict the Maximum Size of Stable Fragments for Acceleration-Induced Breakup of a Liquid Drop*, Int.J.Multiphase Flow, **13**, 741, (1987).

[65] Marmottant P. and Villermaux E., *On Spray Formation*, J. Fluid Mech., **498**, 73-111, (2004).

[66] Ménard T., Demoulin F.X. and Berlemont A., *3D Simulation of the Primary Break-up of a Liquid Jet by Coupling Level Set/VOF/Ghost Fluid Methods*, 6th International Conference on Multiphase Flow, ICMF-2007, Leipzig, Germany, (2007).

[67] Lebas R., Menard T., Beau P.A., Berlemont A. and Demoulin F.X., *Numerical Simulation of Primary Break-up and Atomization: DNS and Modeling Study*, Int. J. Multiphase Flow, **35**, 247-260, (2009).

[68] Sirignano W., *Fluid Dynamics and Transport of Droplets and Sprays*, Cambridge University Press, ISBN-0-521-63036-3, (1999).

[69] Fessler J.R. and Eaton J.K., *Turbulence Modification by Particles in a Backward-Facing Step Flow*, J. Fluid Mech., **394**, 97-117, (1999).

[70] Kenning V.M. and Crowe C.T., *On the Effect of Particles on Carrier Phase Turbulence in Gas-Particle Flows*, Int. J. Multiphase Flow, **23**, 403, (1997).

[71] Wood A.M., Hwang W. and Eaton J.K., *Preferential Concentration of Particles in Homogeneous and Isotropic Turbulence*, Int. J. Multiphase Flow, **31**, 1220-1230, (2005).

[72] Crowe C.T., *On Models for Turbulence Modulation in Fluid-Particle Flows*, Int. J. Multiphase Flow, **26**, 719-727, (2000).

[73] Chen J.H. and Faeth G.M., *Continuous-Phase Properties of Homogeneous Particle-Laden Turbulent Flows*, AIAA Journal, **39**, NO. 1, (2000).

[74] Portela L. and Oliemans R., *Eulerian-Lagrangian DNS/LES of Particle-Turbulence Interactions in Wall-Bounded Flows*, Int. J. Numer. Meth. Fluids, **43**, 1045-1065, (2003).

[75] Poelma C. and Ooms G., *Particle-Turbulence Interaction in a Homogeneous, Isotropic Turbulent Suspension*, Applied Mechanics Reviews, **59**, 78-90, (2006).

[76] Righetti M. and Romano G.P., *Particle-Fluid Interactions in a Plane Near-Wall Turbulent Flow*, J. Fluid Mech., **505**, 93-121, (2004).

[77] Reeks M.W., *On Model Equations for Particle Dispersion in Inhomogeneous Turbulence*, Int. J. Multiphase Flow, **31**, 93-114, (2005).

[78] Hogan R.C. and Cuzzi J.N., *Stokes and Reynolds Number Dependence of Preferential Particle Concentration in Simulated Three-Dimensional Turbulence*, Phys. Fluids, **13**, 2938-2944, (2001).

[79] Jones W.P. and Sheen D.H., *A Probability Density Function Method for Modelling of Liquid Fuel Sprays*, Flow, Turbulence and Combustion **63**, 379-394, (1999).

[80] Vinkovic, I., Aguirre C., Simoens S. and Gorokhovski M., *Large Eddy Simulation of Droplet Dispersion for Inhomogeneous Turbulent Wall Flow*, Int. J. Multiphase Flow, **32**, 344-364, (2006).

[81] Elghobashi S., *On Predicting Particle-Laden Turbulent Flows*, Applied Scientific Research, 48, 301-314, (1991).

[82] Elghobashi S., *Particle-Laden Turbulent Flows: Direct Simulation and Closure Models*, Applied Scientific Research, 52, 309-329, (1994).

[83] $http://www.opencfd.co.uk/$ and the references therein (2007).

[84] $http://openfoamwiki.net/index.php/OpenFOAMReferences$ and the references therein (2007).

[85] $www.ltt-rostock.de/mediawiki/index.php/Xoodles$ and the references therein (2008).

[86] Jasak H., *Error Analysis and Estimation for the Finite Volume Method with Applications to Fluid Flows*, PhD thesis, Imperial College, London, (1996).

[87] Guenther R.B. & Lee J.W., *Partial Differential Equations of Mathematical Physics and Integral Equations*, Dover Publications, Inc., New York, ISBN-0-486-68889-5, (1996).

[88] Canuto C., Hussaini M.Y., Quarteroni A. & Zang T.A., *Spectral Methods - Evolution to Complex Geometries and Applications to Fluid Dynamics*, ISBN-978-3-540-30727-3, Springer-Verlag Berlin Heidelberg (2007).

[89] Rade L. and Westergren B., Mathematics Handbook for Science and Engineering, Student Litteratur, ISBN 91-44-00839-2, (1999).

[90] Burattini P. and Djenidi L., *Velocity and Passive Scalar Characteristics in a Round Jet with Grids at the Nozzle Exit*, Flow, Turbulence and Combustion **72**, 199-218, (2004).

[91] Burattini P., Antonia R.A., Rajagopalan S. and Stephens M., *Effect of Initial Conditions on the Near-Field Development of a Round Jet*, Experiments in Fluids, **37**, 56-64, (2004).

[92] Ding R., *Experimental Studies of Turbulent Mixing in Impinging Jets*, PhD Thesis, Lund, Sweden, ISBN-91-628-6201-4, (2004).

[93] Örlü R., *Investigation of the Near Field of a Swirling Turbulent Jet*, Licentiate's thesis, KTH, Stockholm, (2006).

[94] Danaila I. and Boersma B.J., *Direct Numerical Simulation of Bifurcating Jets*, Phys. Fluids, **12**, 1255-1257, (2000).

[95] Shraiman B.I. and Siggia E.D., *Scalar Turbulence*, NATURE, **405**, 8, (2000).

[96] Dimotakis P.E., *Turbulent Mixing*, Annu.Rev.Fluid Mech., **37**, 329-356, (2005).

[97] Aggarwal S.K., *A Review of Spray Ignition Phenomena: Present Status and Future Research*, Prog. Energy Combust. Sci., **24**, 565-600, (1998).

[98] Edwards C., Siebers D. and Hoskin D., *A Study on the Autoignition Process of a Diesel Spray via High Speed Visualization*, SAE Technical Paper Series 920108, (1992).

[99] Kundu P. and Cohen I., *Fluid Mechanics*, Academic Press, ISBN 978-0-12-373735-9, (2008).

[100] Borman G. and Ragland K. *Combustion Engineering*, McGraw International Editions, ISBN 0-07-115978-9, (1998).

[101] Jeong J. and Hussain F., On the Identification of a Vortex, J.Fluid Mech., **285**, 69-94, (1995).

ISBN 978-952-60-3165-1
ISBN 978-952-60-3166-8 (PDF)
ISSN 1795-2239
ISSN 1795-4584 (PDF)